

^{13}C -Satellite Decoupling Strategies for Improving Accuracy in Quantitative NMR

Adilah Bahadoor,^{*,†} Andreas Brinkmann,[†] and Jeremy E. Melanson[†]

[†]Metrology, National Research Council Canada, Ottawa, ON K1A 0R6, Canada

Table of Contents

Title-Supporting Information Figures	Page
Experimental	S3-S4
Fig S1. The effect of pulse length (pcpd2) and decoupling power levels (pW12) on ^{13}C -decoupling.	S5
Fig S2. The effect of o2p during bi-level adiabatic decoupling.	S6
Fig S3. The power levels for a WURST-20 bi-level adiabatic pulse was explored at 400 MHz.	S7
Fig S4. The actual temperatures recorded for the Bruker thermometer sample with D1 = 60s and D1= 6s respectively, during ^1H -NMR, $^1\text{H}\{^{13}\text{C}\}$ -NMR via GARP and $^1\text{H}\{^{13}\text{C}\}$ -NMR via a WURST-20 bi-level adiabatic decoupling.	S8
Fig S5. The determination of the optimal acquisition time for $^1\text{H}\{^{13}\text{C}\}$ -NMR at 400 MHz	S9
Fig S6. The theoretical NOE enhancements expected during $^1\text{H}\{^{13}\text{C}\}$ -NMR for an isolated ^1H - ^{13}C system.	S10
Fig S7. NOE enhancements observed for a sample of $^{13}\text{C}_6$ -tyrosine in D_2O during inverse-gated ^{13}C -decoupling vs continuous ^{13}C -decoupling	S11
Fig S8. Approximate graphical representation of NOE build-up and decay.	S12
Fig S9. Observed NOEs for protons involved in ^1H - ^{13}C bonding during $^1\text{H}\{^{13}\text{C}\}$ -NMR via inverse gated or gated decoupling	S13
Fig S10. Three replicate qHNMR spectra of dimethyl terephthalate and benzoic acid in acetone-d6 at 400 MHz.	S14
Fig S11. Three replicate qH $\{^{13}\text{C}\}$ NMR spectra of dimethyl terephthalate and benzoic acid in acetone-d6 via GARP decoupling and WURST-20 bi-level adiabatic decoupling at 400 MHz.	S15
Fig S12. Three replicate qHNMR and qH $\{^{13}\text{C}\}$ NMR spectra of dimethyl terephthalate and benzoic acid in acetone-d6 recorded at 900 MHz.	S16
Fig S13. The ^{13}C -spectrum of DMT + BA in acetone-d6 recorded at 400 MHz.	S17
Fig S14. Three replicate qHNMR spectra of angiotensin-II and maleic acid in D_2O at 400 MHz.	S18
Fig S15. Three replicate qH $\{^{13}\text{C}\}$ NMR spectra of angiotensin II and maleic acid in D_2O via GARP decoupling and WURST-20 bi-level adiabatic decoupling obtained at 400 MHz.	S19
Fig S16. Three replicate qHNMR and qH $\{^{13}\text{C}\}$ NMR spectra of angiotensin II and maleic acid in D_2O recorded at 900 MHz.	S20
Fig S17. The HSQC spectrum of angiotensin II + maleic acid in D_2O at 400 MHz.	S21
Fig S18. The overlay of the ^1H -NMR spectra of zearalenone (ZEA) over zearalanone (ZAN).	S22
Fig S19. The overlay of the GARP-mediated $^1\text{H}\{^{13}\text{C}\}$ -NMR spectra of zearalenone (ZEA) over zearalanone (ZAN)	S23
Fig S20. Three replicate $^1\text{qHNMR}$ and GARP-mediated qH $\{^{13}\text{C}\}$ NMR spectra of zearalenone (analyte) and dimethyl terephthalate (calibrant) in acetone-D ₆ recorded at 400 MHz	S24
Fig S21. The ^1H -NMR and GARP-mediated $^1\text{H}\{^{13}\text{C}\}$ -NMR spectra of $^{13}\text{C}_6$ -ochratoxin A in CD_3CN + 0.1% DCOOH and CD_3OD respectively.	S25
Fig S22. Monitoring the doublet for the methyl group at position 21 for signs of tautomerization when $^{13}\text{C}_6$ -ochratoxin A was dissolved in CD_3CN + 0.1% DCOOH .	S26
Fig S23. Three replicate qHNMR spectra of $^{13}\text{C}_6$ -ochratoxin A with maleic acid as the external standard.	S27
Fig S24. Three replicate qH $\{^{13}\text{C}\}$ NMR spectra of $^{13}\text{C}_6$ -ochratoxin A with maleic acid as the external standard.	S28
Title-Supporting Information Tables	
Table S1. The % standard deviation of integral replicates for zearalenone and $^{13}\text{C}_6$ -ochratoxin A.	S28
Table S2. The corrected integrals for H(5) + H(4, 6) of benzoic acid.	S14
Table S3. The corrected integrals for MA H(2, 3) and Tyr H(3, 5) of angiotensin II.	S18
Purity calculations and ANOVA comparisons:	
The purity of dimethyl terephthalate (analyte) with benzoic acid (internal calibrant) at 400 and 900 MHz	S30-S31
The ANOVA: Single factor comparison for purity values of dimethyl terephthalate at 400 and 900 MHz	S31
The purity of angiotensin II (analyte) with maleic acid (internal calibrant) at 400 MHz	S32-S33
The ANOVA: Single factor comparison for purity values of angiotensin II at 400 MHz	S33
The purity of angiotensin-II (analyte) with maleic acid (internal calibrant) at 900 MHz	S34
The ANOVA: Single factor comparison for purity values of angiotensin II at 900 MHz	S34
The purity of zearalenone (analyte) with dimethyl terephthalate (internal calibrant) at 400 MHz	S35
The ANOVA: Single factor comparison for purity values of zearalenone at 400 MHz	S35
The concentration of $^{13}\text{C}_6$ -ochratoxin A (analyte) with maleic acid as external calibrant for Sample 1	S36
The ANOVA: Single factor comparison between qHNMR and GARP decoupling data for $^{13}\text{C}_6$ -ochratoxin A sample 1	S37
The concentration of $^{13}\text{C}_6$ -ochratoxin A (analyte) with maleic acid as external calibrant for Sample 2	S38
The ANOVA: Single factor comparison between qHNMR and GARP decoupling data for $^{13}\text{C}_6$ -ochratoxin A sample 2	S39
References	S40

Experimental

Chemicals. Maleic acid and dimethyl terephthalate were obtained from the Trace-CERT line of qNMR standards from Sigma-Aldrich (St. Louis, MO). Benzoic acid PS-1 and KHP 84L were provided by NIST (Gaithersburg, MD). $^{13}\text{C}_6$ -ochratoxin A was synthesized in-house.¹ Angiotensin-II was purchased from Anaspec, CA, USA. Zearalenone was provided by Agriculture and Agri-Food Canada. The deuterated NMR solvents, CD_3CN , D_2O , $(\text{CD}_3)_2\text{CO}$ and the acid modifier DCOOH were purchased from Cambridge Isotope Labs, MA. All chemicals and reagents were used as obtained.

Sample Preparations for qNMR. All samples were gravimetrically prepared in a temperature and humidity controlled balance room on a Mettler-Toledo XP-6U microbalance that was exercised and mass calibrated on the same day. Analyte and standard samples were directly weighed in pre-washed and dried 2 mL Wheaton glass vials.

NMR Experimental Set-Up. All samples were analyzed in triplicate at 20 °C. For most samples, T_1 for the longest relaxing nuclei was determined by an inverse recovery experiment (pulse sequence “t1ir”) and the relaxation delay (D1) was set at $10 \times T_1$. Since the time interval $5.5 \text{ s} \leq T_1 \leq 6 \text{ s}$ was a common denominator for a majority of samples used in this report, D1 was set at 60 s by default, if T_1 was not individually determined. For each sample, the 90° pulse (p1) was estimated from the 360° null point at the onset of the experiment and used for all replicate acquisitions. In general, an approximate pulse length (p1) of 13.3 μs was common for samples analyzed at 400 MHz. At 900 MHz, a shorter p1 value of 9 – 9.5 μs was common. The number of accumulated scans depended on the sample concentration. In general, no less than 16 scans were recorded and 2 dummy scans (DS) were deemed sufficient to achieve a steady state, prior to FID accumulation for ^1H -NMR. For $^1\text{H}\{^{13}\text{C}\}$ -NMR, 4 – 6 dummy scans were optimal. Quantitative ^1H -NMR acquisitions were performed at 128k data points over a 30 ppm sweep width, which resulted in an acquisition time of 5.4 s. The acquisition time for quantitative $^1\text{H}\{^{13}\text{C}\}$ -NMR was dictated by the FID decay profile of the sample. An acquisition time of 2.5-2.7 s was the routine starting point. If truncation of the FID was observed, the acquisition time was increased accordingly, typically up to 5 s.

GARP-Mediated ^{13}C -decoupling procedures. The GARP-mediated $^1\text{H}\{^{13}\text{C}\}$ NMR was adapted from the inverse gated Bruker pulse sequence ‘zgif’. A 90° ^{13}C decoupling pulse length (pcpd2) of 80 μsec at 0.91 W was applied via the decoupler channel. Lower power 90° ^{13}C decoupler pulse calibration was performed for the parameter “plw12” using the parameter optimization program “popt” for the pre-set pulse length (pcpd2) of 80 μsec on the Bruker standard sample (1% CHCl_3 in acetone- d_6). In general, fine adjustments to the decoupler pulse length/power level were not critical, as slight offsets still provided complete decoupling (Supp. Info. Fig S1). The decoupler offset in the F2 dimension (^{13}C nucleus) was set at 80 ppm, thus enabling broadband decoupling over a sweep width of 160 ppm. The chemical shifts of most protonated sp^2 -hybridized carbons safely fit within a 160 ppm window to include the aromatic region. Often a less crowded region of the spectrum, it offers distinct aromatic signals that are attractive targets for integration, as long as these signals are not exchangeable. Point in case, aromatic signals are usually the integrals of choice during the quantitative NMR analysis of small peptides, as clearly illustrated by the qHNMR and $^1\text{H}\{^{13}\text{C}\}$ NMR quantitation of angiotensin II (*vide infra*).

Bi-level Adiabatic Decoupling Procedures. To set up bi-level adiabatic decoupling on a 400 MHz spectrometer, a high-power WURST-20 pulse (shaped pulse power: 0.79 W, duration: 1 ms, sweepwidth: 18 KHz or 180 ppm) and a low power WURST-20 (shaped pulse power: 0.40 W, duration: 2 ms, sweepwidth: 18 KHz) were implemented with the five-step phase cycle (0°, 150°, 60°, 150°, 0°).⁵⁰ Choosing an optimal frequency offset (o2p) for each sample was best. The shaped Wurst-20 pulses were created with Shape Tool. Setting o2p close to the center of the region to be decoupled ensured all signals within this region are subject to near equal irradiation for complete decoupling. Thus, for a standard Bruker sample of 3% CHCl_3 + 0.2% TMS in acetone- d_6 , incomplete decoupling of the TMS peak was observed when o2p was set at 100 ppm (Supp. Info Figs. S2A-S2B). With o2p at 40 ppm, the mid-point between the ^{13}C signals for CHCl_3 at 80 ppm and TMS at 0 ppm, full decoupling of all ^{13}C -satellites was observed (Supp. Info Fig. S2C). The calibrated power levels of both the 2 ms low power shaped pulse and the 1 ms high power shaped pulse were obtained for the parameter “SPW3” from parameter optimization “popt” on the pulse program “dec180sp” using the 3% CHCl_3 + 0.2% TMS in acetone- d_6 sample. The calibrated power level was the power which produced the minimal ^{13}C -satellite signal for CHCl_3 at the chosen pulse length. It should be noted that decoupling at powers slightly less than the determined calibrated power levels still functioned well (Supp. Info Fig. S3). The 90° inverse-gated pulse sequence “zgif” was used to acquire all $^1\text{H}\{^{13}\text{C}\}$ -qNMR spectra via the WURST-20 bi-level adiabatic decoupling scheme described.

On the 900 MHz spectrometer, a high-power Chirp-32 pulse (shaped pulse power: 5.75 dB (20 W), duration: 1.5 ms, sweepwidth: 32 KHz or 140 ppm) and a low power Chirp-32 (shaped pulse power: 11.77 dB (5 W), duration: 3 ms, sweepwidth: 32 KHz) were implemented with the five-step phase cycle (0°, 150°, 60°, 150°, 0°).⁵⁰ The Chirp-32 pulse was used as from the Bruker library, but the power was optimized separately. To determine the lowest optimal decoupling power, the power was incrementally reduced from the default “getprosol” values until cycling sidebands appeared in the $^1\text{H}\{^{13}\text{C}\}$ -qNMR spectrum. The presence of cycling sidebands was an indication that the decoupling power was too low. The calibrated decoupling power levels that was adopted was the minimum power levels at which cycling sidebands were no longer observed. The Chirp-32 bi-level adiabatic decoupling scheme was implemented within a 30° inverse-gated pulse “zgif30”.

Processing procedures. All spectra were processed with Topspin 3.6, zero-filled to 128k and exponentially multiplied at a line broadening of 0.3 Hz before phasing manually. A manual polynomial baseline correction was performed along spectral segments containing integrals of interest before integrating. This segmented approach to baseline correction was more effective in producing a flatter baseline, than correcting the baseline over the full spectrum (usually about 10 ppm).

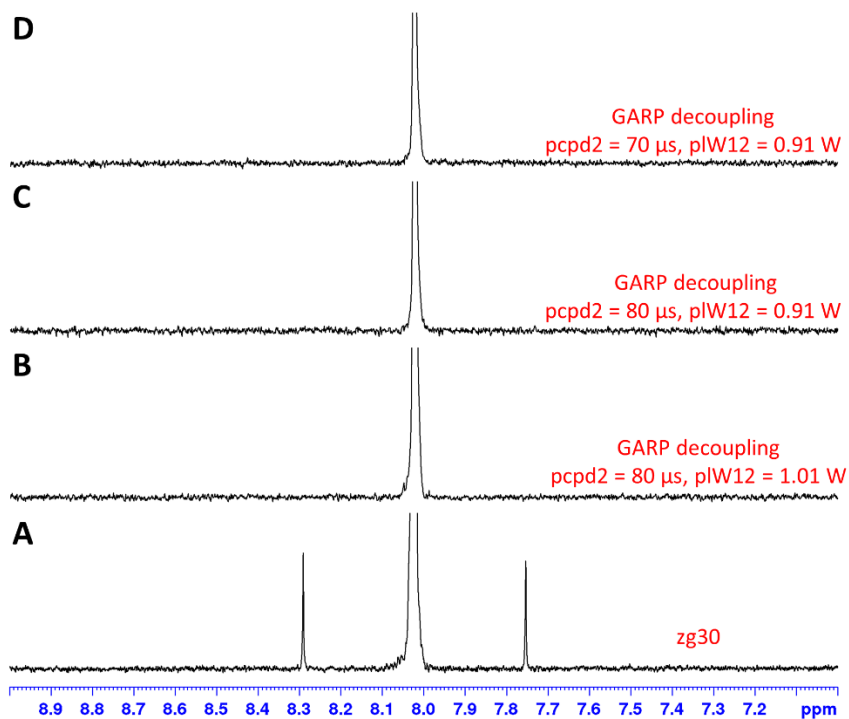


Figure S1. The effect of pulse length (pcpd2) and decoupling power levels (pIW12) on ^{13}C -decoupling were explored with a standard Bruker sample of 1% CHCl_3 in acetone- d_6 . **(A)** Without decoupling the ^{13}C -satellites of CHCl_3 were clearly observed. **(B)** GARP decoupling at 1.01 W over a pulse length of 80 μ s effectively decoupled all the ^{13}C -satellites of CHCl_3 . **(C)** Keeping the pulse length unchanged at 80 μ s, while reducing PL12 to 0.91 W was just as effective in decoupling the ^{13}C -satellites. **(D)** Complete ^{13}C -satellite decoupling was also observed when the power level was maintained at 0.91 W, while shortening pulse length to 70 μ s.

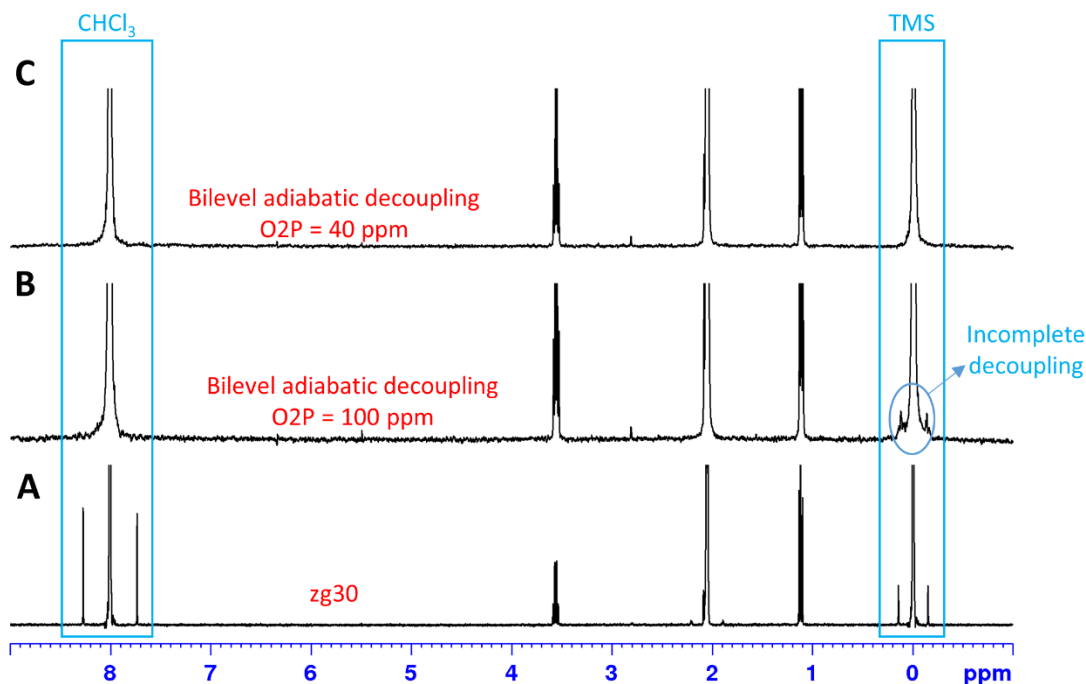


Figure S2. The effect of o2p during bi-level adiabatic decoupling (high power pulse duration of 1500 μ s, over a 22 KHz sweep width, at a power of 0.79W and low power pulse duration of 3000 μ s, over a 22 KHz sweep width, at a power of 0.40 W) was explored with a standard Bruker sample of 3% CHCl_3 and 0.2% TMS at 400 MHz. **(A)** Without decoupling the ^{13}C -satellites of CHCl_3 and TMS were clearly observed. **(B)** With o2p at 100 ppm, the ^{13}C -satellites of CHCl_3 were effectively decoupled, while visible sidebands around the TMS signal indicated that its ^{13}C -satellites were poorly decoupled. **(C)** When o2p was shifted up-field to 40 ppm, ^{13}C -satellites of both CHCl_3 and TMS were fully decoupled.

NOTE: The sweep width was eventually reduced to 18 KHz from 22 KHz and the durations for the pulses were reduced to 1000 μ s (high power) and 2000 μ s (low power) for more effective and reproducible ^{13}C -decoupling. These optimal conditions for WURST-20 bi-level adiabatic decoupling are illustrated for dimethyl terephthalate and angiotensin II acquired at 400 MHz described in Figs. S10B and S13B respectively.

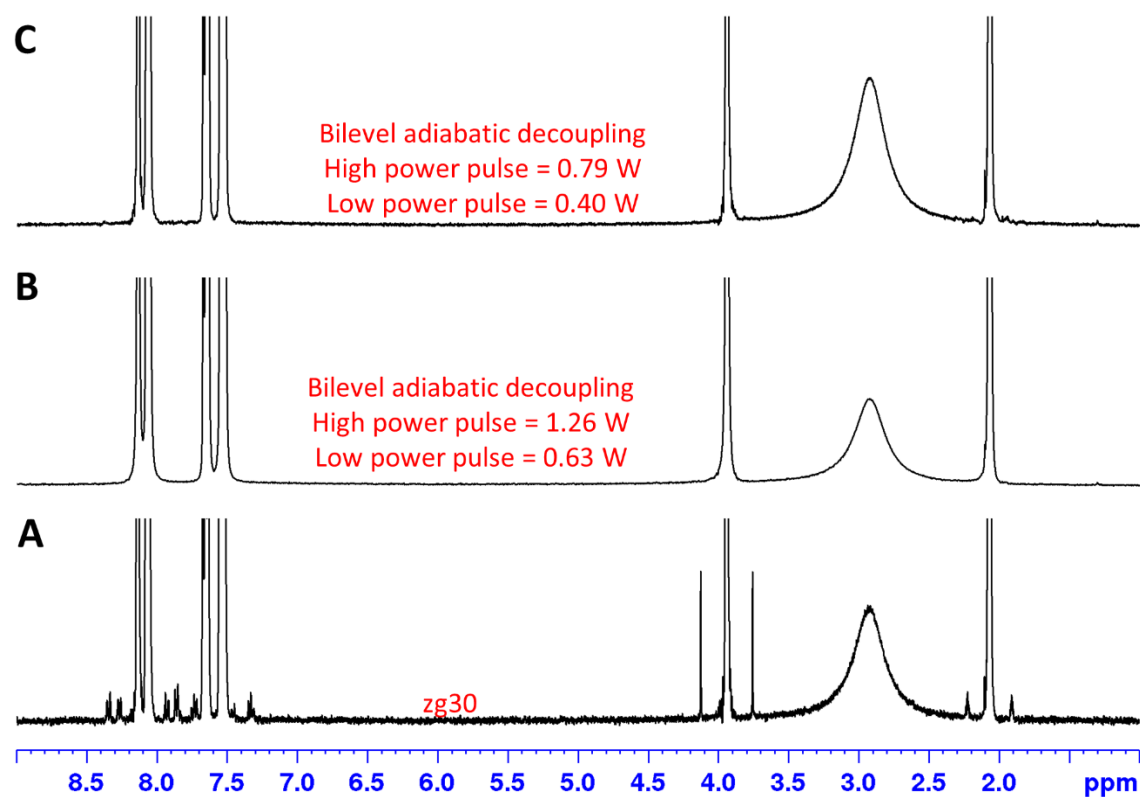


Figure S3. The power levels for a WURST-20 bi-level adiabatic pulse (high power pulse duration of 1000 μ s, over 18 KHz sweep width and a low power pulse duration of 2000 μ s, over 18 KHz sweep width) was explored at 400 MHz with a sample of benzoic acid and dimethyl terephthalate in acetone- d_6 for which the optimal ω_{2p} was 95 ppm. **(A)** Without decoupling the ^{13}C -satellites of all the proton signals were clearly observed. **(B)** All the ^{13}C -satellites were effectively decoupled at high/low power combination of 1.26W and 0.63 W, the calibrated power levels from “popt”. **(C)** Full ^{13}C -satellite decoupling was still observed even when the high/low power combination was reduced to 0.79W and 0.40W.

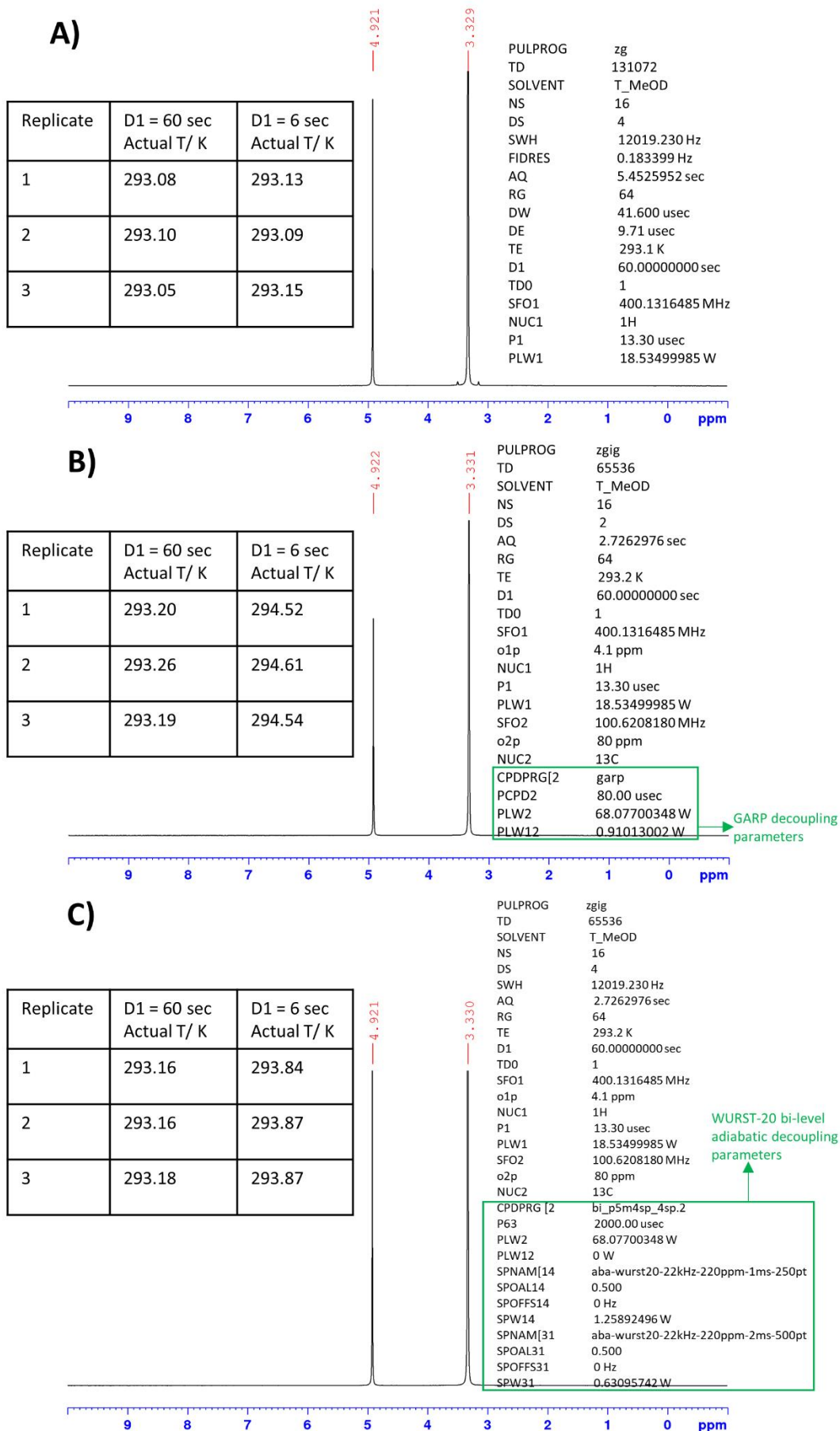
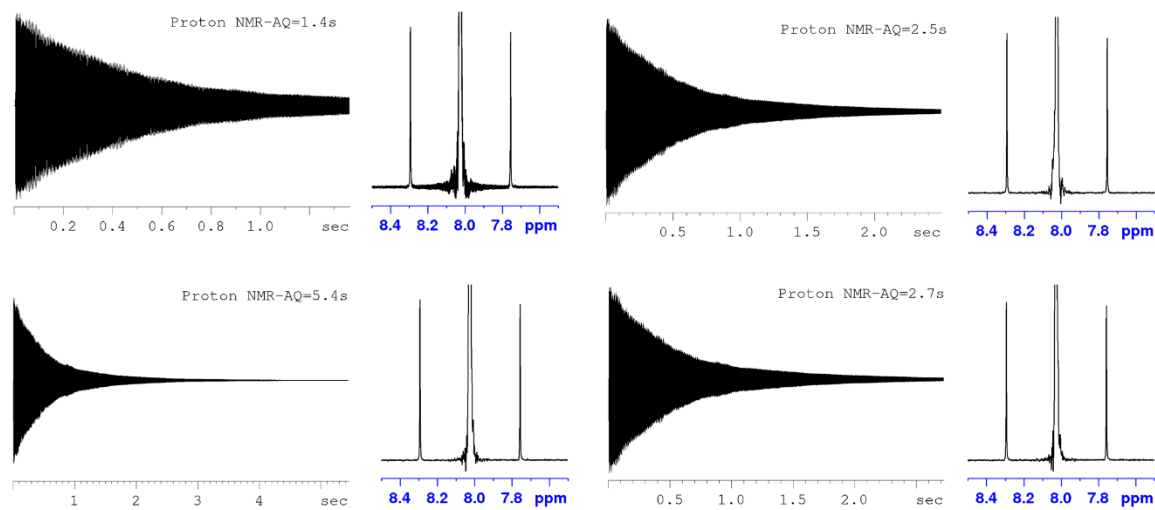


Figure S4. The actual temperatures recorded for the Bruker thermometer sample with D1 = 60s and D1= 6s respectively, during acquisition via **(A)** ^1H -NMR, **(B)** $^1\text{H}\{^{13}\text{C}\}$ 8p-NMR via GARP and **(C)** $^1\text{H}\{^{13}\text{C}\}$ -NMR via a bi-level adiabatic decoupling.

A) FID decays and respective processed spectra as a function of acquisition time during ^1H -NMR.



B) FID decays and respective processed spectra as a function of acquisition time during $^1\text{H}\{^{13}\text{C}\}$ -NMR.

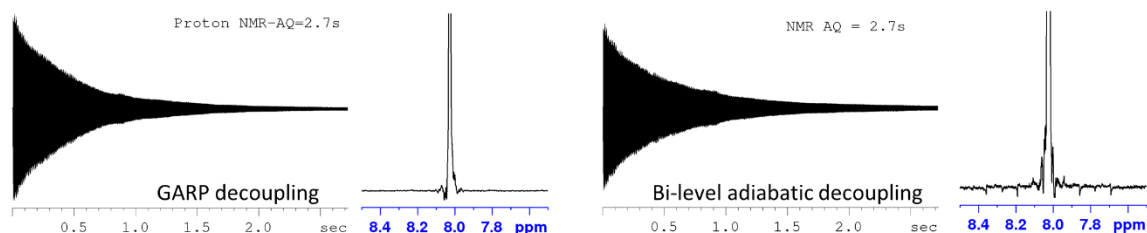


Figure S5. The determination of the optimal acquisition time for $^1\text{H}\{^{13}\text{C}\}$ -NMR at 400 MHz using a standard Bruker sample of 3% CHCl_3 + 0.2% TMS, showing the CHCl_3 peak only at 8 ppm. **(A)** For ^1H -NMR, acquisition times of 1.4 and 5.4 s were the two extremes producing a partially or fully decayed FID respectively. Near complete decay was obtained when the acquisition time was shortened to 2.5/2.7 s to produce a spectrum that did not exhibit any telltale signs of truncation (*as seen from the spectrum acquired at 1.4 s*) and looked very similar to the processed spectrum obtained with a long AQ of 5.4 s. **(B)** An acquisition time of 2.5/2.7 s produced good peak shapes during $^1\text{H}\{^{13}\text{C}\}$ -NMR without major signs of truncation.

Acquisition parameters for:

GARP: 80 μs pulse at 0.91 W, o2p = 80ppm, o1p = 5ppm, pulse sequence = zgig

Bi-level adiabatic decoupling: high power WURST-20 pulse (1.5 ms, 0.79W, 160ppm), low power WURST-20 pulse (3 ms, 0.16 W, 160ppm), o2p = 80ppm, o1p = 5ppm, pulse sequence = zgig

Processing parameters: Window function = em, LB = 0.3

NOTE: the decoupling power and duration for the WURST-20 pulses were not fully optimized yet when this experiment was performed. Thus, cycling sidebands centered from the main CHCl_3 signal as observed during bi-level adiabatic decoupling in Fig S5B, are a result of these sub-optimal decoupling parameters.

The general equation for heteronuclear steady state NOEs for an isolated 2-spin system:²

$$\eta\{S\} = \frac{\gamma_S}{2\gamma_I}$$

Where $\eta\{S\}$ = NOE induced for spin I when spin S is perturbed and γ_S = gyromagnetic ratio for spin S and γ_I = gyromagnetic ratio for spin I.

Hence for $^1\text{H}\{^{13}\text{C}\}$ -NMR, a theoretical maximum NOE enhancement of 12% for ^1H is predicted, when ^{13}C is perturbed:

$$\eta\{S\} = \frac{\gamma_{^{13}\text{C}}}{2\gamma_{^1\text{H}}} = \frac{10.71}{2 * 42.58} = 0.12$$

Where $\gamma_{^{13}\text{C}} = 10.71 \text{ MHz/T}$; $\gamma_{^1\text{H}} = 42.58 \text{ MHz/T}$

The actual probability of encountering NOE enhancement during $^1\text{H}\{^{13}\text{C}\}$ -NMR is 0.13%:

The natural abundance of $^{13}\text{C} = 1.1\%$.

This low abundance reduces the chances of NOE enhancement for ^1H during $^1\text{H}\{^{13}\text{C}\}$ -NMR to $0.011 * 12\% = 0.13\%$

Figure S6. The theoretical NOE enhancements expected during $^1\text{H}\{^{13}\text{C}\}$ -NMR for an isolated ^1H - ^{13}C system.

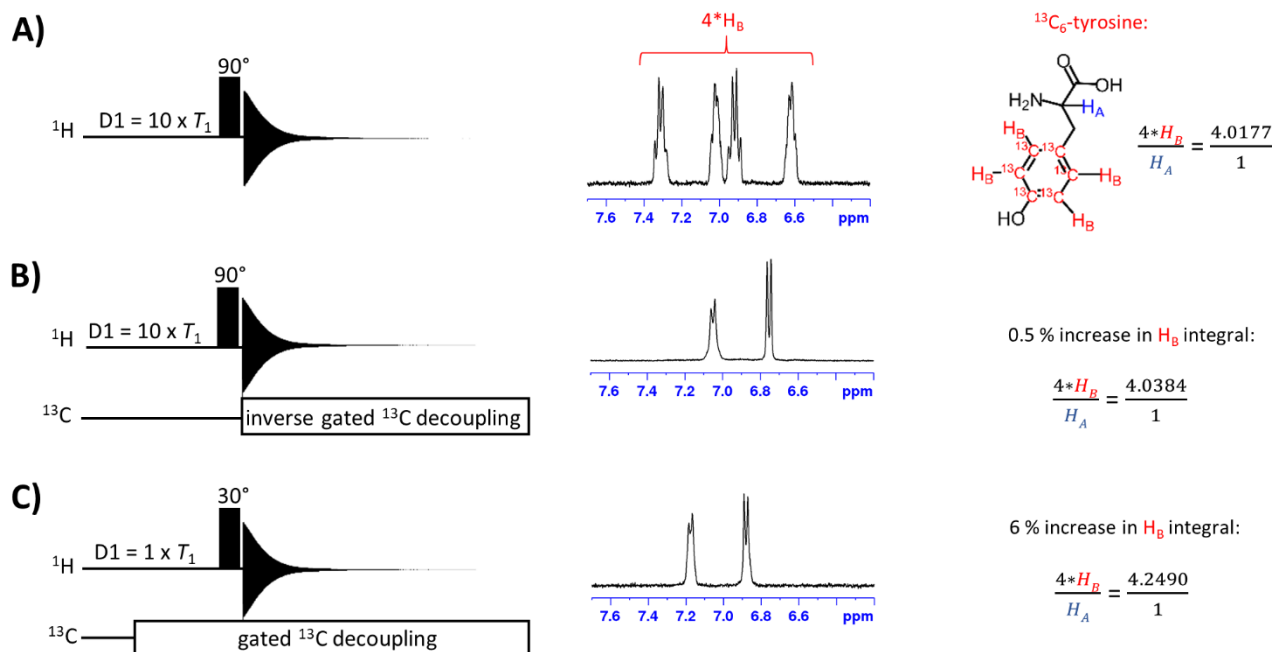


Figure S7. NOE enhancements observed for a sample of $^{13}\text{C}_6$ -tyrosine in D_2O during inverse-gated ^{13}C -decoupling vs continuous ^{13}C -decoupling. (A) No NOE enhancements were expected during ^1H -qNMR, thus providing the reference value for the integral for H_B . (B) The ^{13}C -satellites for H_B were fully decoupled during inverse-gated $^1\text{H}\{^{13}\text{C}\}$ -qNMR producing a minimal 0.5% increase in the integral compared to ^1H -qNMR, when $D1$ was fixed at 60 s or $10 * T_1$. (C) A 6% increase in the integral for H_B was observed during continuous ^{13}C -decoupling (note that the delay of $1 * T_1$ and a 30° pulse were used during continuous decoupling to prevent overheating of the probe and sample).

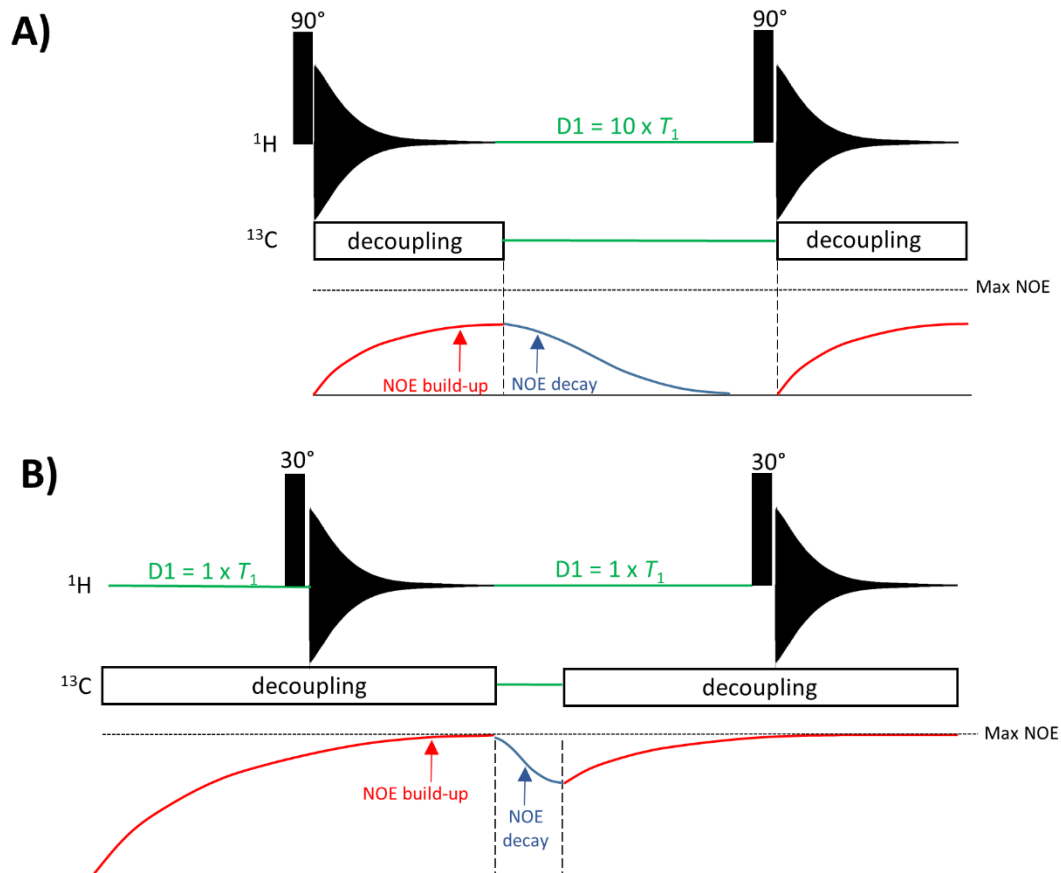


Figure S8. Approximate graphical representation of NOE build-up and decay.²⁻³ **(A)** During inverse gated decoupling, the NOE builds up during acquisition only. Because this interval is short (usually $< 3\text{s}$), the NOE most likely cannot reach its maximum value before it starts to decay. If the relaxation delay ($D1$) between successive acquisitions spans at least $10 \times T_1$, the accumulated NOE has enough time to decay to zero. **(B)** The decoupler is turned on during the delay and the acquisition time in a continuous decoupling set up. This duration may be long enough for the NOE to reach its maximum value. However, the lag time between each decoupling interval is short and the NOE does not fully decay before it starts to accumulate again.

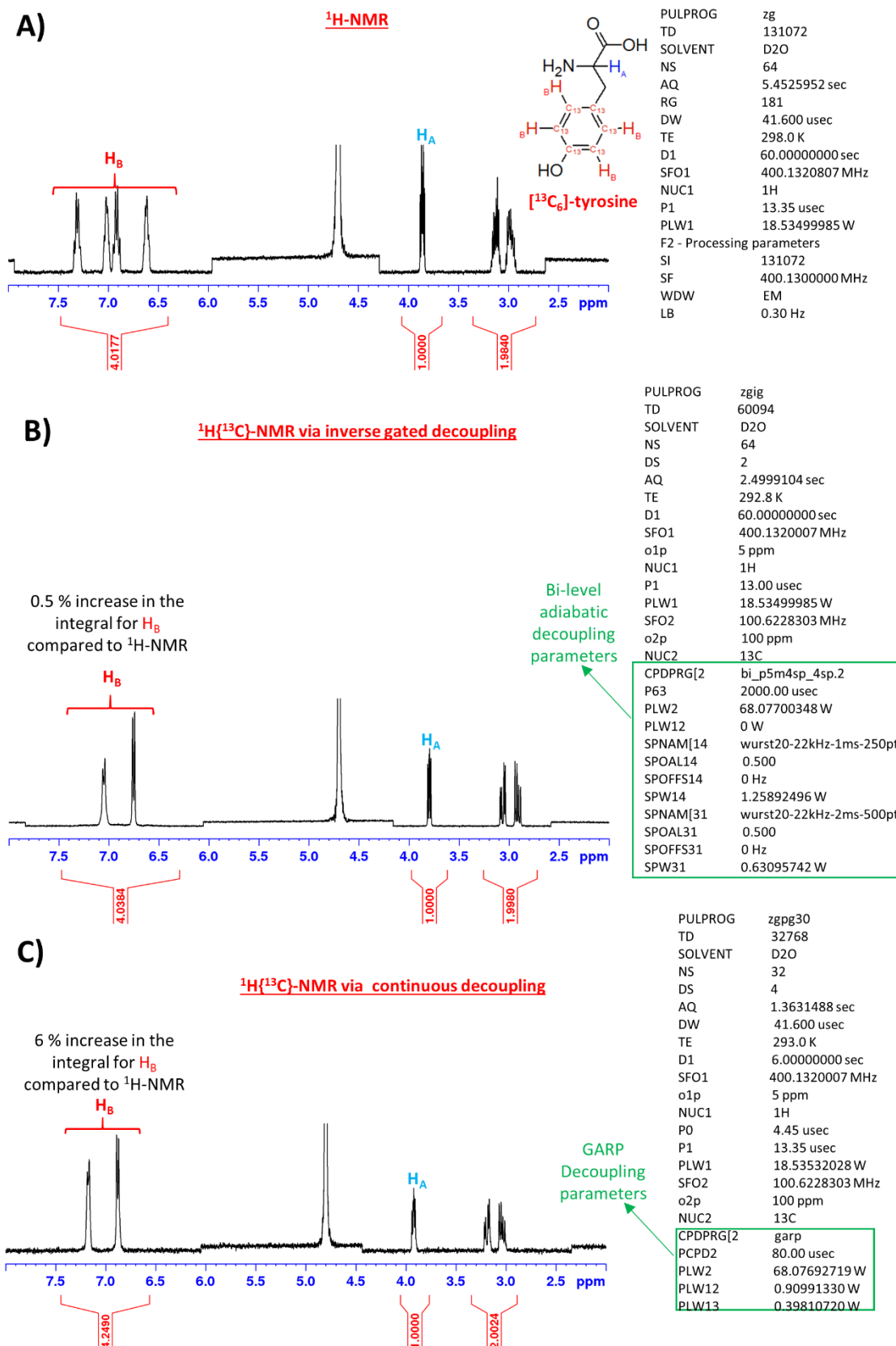


Figure S9. Observed NOEs for protons involved in ^1H - ^{13}C bonding during $^1\text{H}\{^{13}\text{C}\}$ -NMR via inverse gated or continuous decoupling, on a sample of $^{13}\text{C}_6$ -tyrosine in D_2O . To compare integral values, the H_B integrals in each spectrum were normalized to the integral for H_A (set to 1). (A) One bond coupling between ^1H and ^{13}C on the aromatic ring produces the ^{13}C -satellites as the major peaks for H_B in the ^1H -NMR spectrum. (B) Inverse gated ^{13}C decoupling produced a negligible increase of 0.5% in the integral for H_B during $^1\text{H}\{^{13}\text{C}\}$ -NMR. (C) A significant increase of 6% in the integral for H_B was obtained during $^1\text{H}\{^{13}\text{C}\}$ -NMR via continuous decoupling. **Note** that D1 and AQ were shortened to 6 s and 1.36 s respectively to prevent undue probe heating at longer durations.

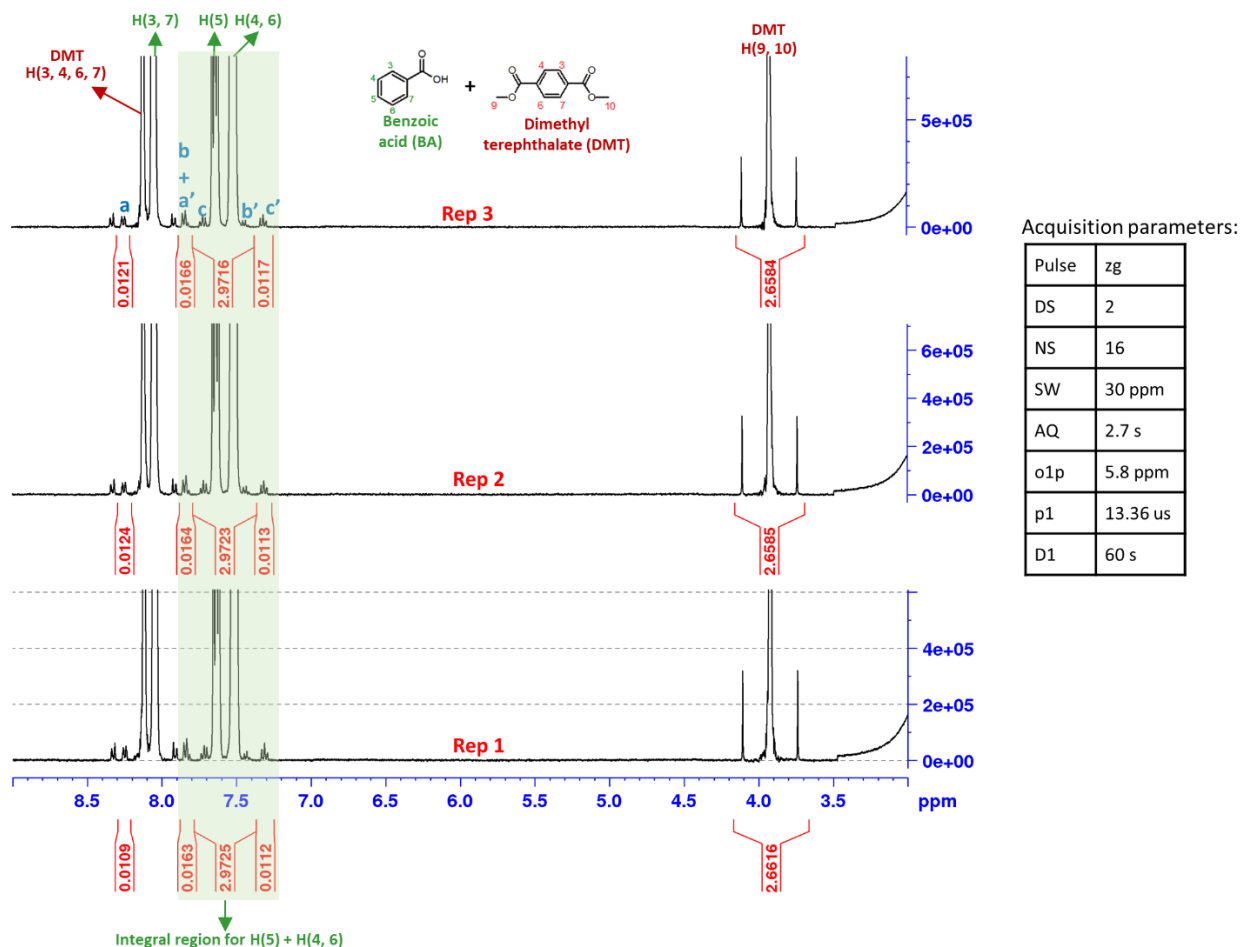


Figure S10. Three replicate ^1H -qNMR spectra of DMT (analyte) and BA (internal standard) in acetone- d_6 recorded at 400 MHz. For BA, the ^{13}C -satellites of H(3, 7) were ($a + a'$), ($b + b'$) for H(5) and ($c + c'$) for H(4, 6). The accurate integral for H(5) + H(4, 6) should include the integrals for ($b + b'$) and ($c + c'$). The integral for a' interfered with b . To obtain an accurate integration for H(5) + H(4, 6), a correction for a' was performed (*vide infra* and **Table S2**). Please see pg. S25 for purity calculations.

The total integral for H(5) + H(4, 6) was set to 3.

$$\therefore \text{corrected integral for H(5) + H(4, 6)} = 3 - a'$$

To obtain a value for a' , a normalized value for one ^{13}C -satellite was determined.

$$\text{Normalized integral} = \frac{(a + (b + a') + c')}{7}$$

where $a' = 2 \times ^{13}\text{C-H}(3, 7)$, $(b + a') = [1 \times ^{13}\text{C-H}(5) + 2 \times ^{13}\text{C-H}(3, 7)]$ and $c' = 2 \times ^{13}\text{C-H}(4, 6)$. The integrals for a' , $(b + a')$ and c' were chosen because they were distinct. **NOTE:** although in theory $a = a'$ and a could be clearly integrated in the spectra shown above, experimentally it was very difficult to obtain similar integrals for two juxtaposed satellites. Therefore, determining a normalized value for one $^{13}\text{C-H}$ was deemed to be more representative of the experimental value.

$$\text{Average integral for } a' = 2 \times \text{normalized } ^{13}\text{C satellite integral}$$

Table S2. The corrected integrals for H(5) + H(4, 6) of benzoic acid.

	$a' + (b + a') + c'$	Normalized ^{13}C -satellite integral	Total Integral H(5) + H(4, 6)	Corrected integral for H(5) + H(4, 6)
Rep 1	0.0384	0.005485714	3.0000	2.989028571
Rep 2	0.0401	0.005728571	3.0000	2.988542857
Rep 3	0.0404	0.005771429	3.0000	2.988457143

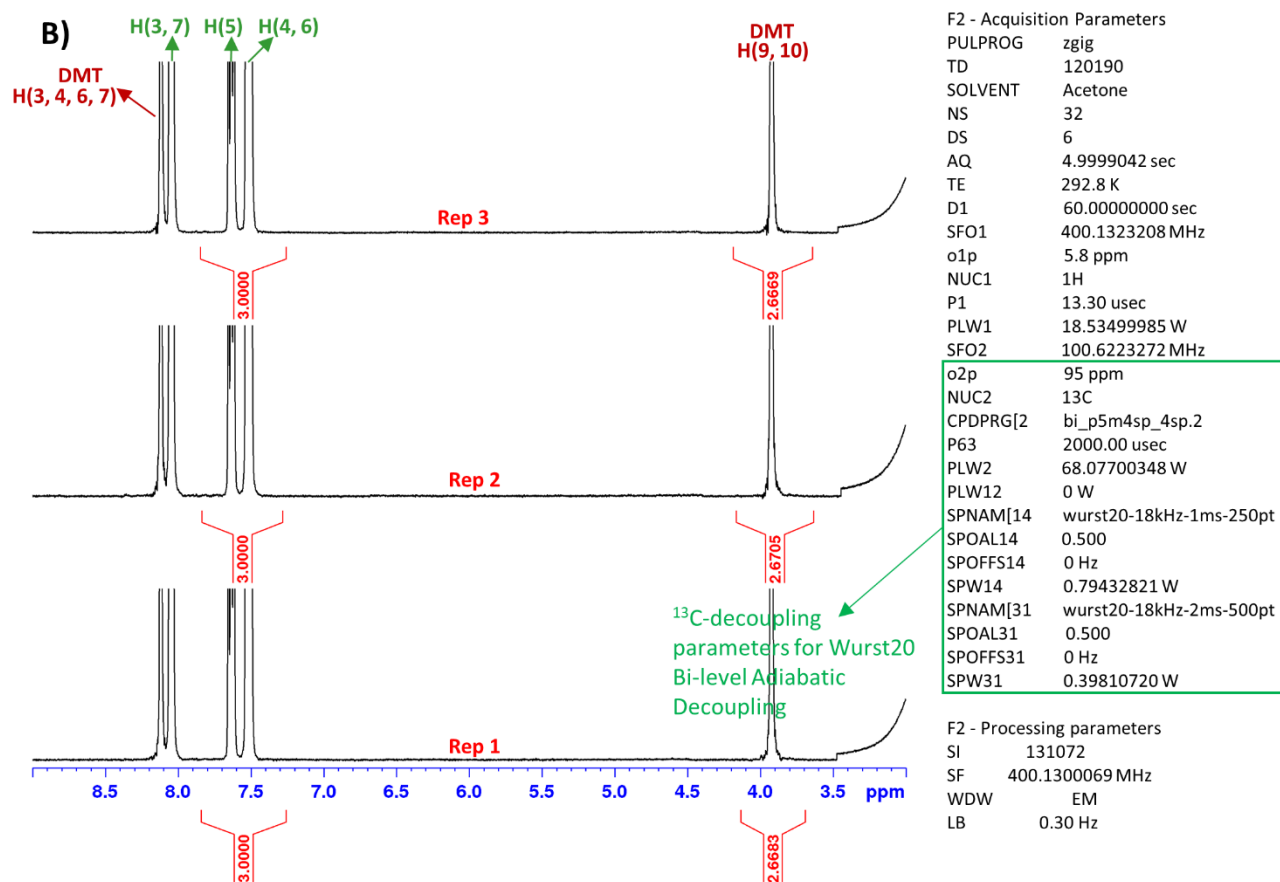
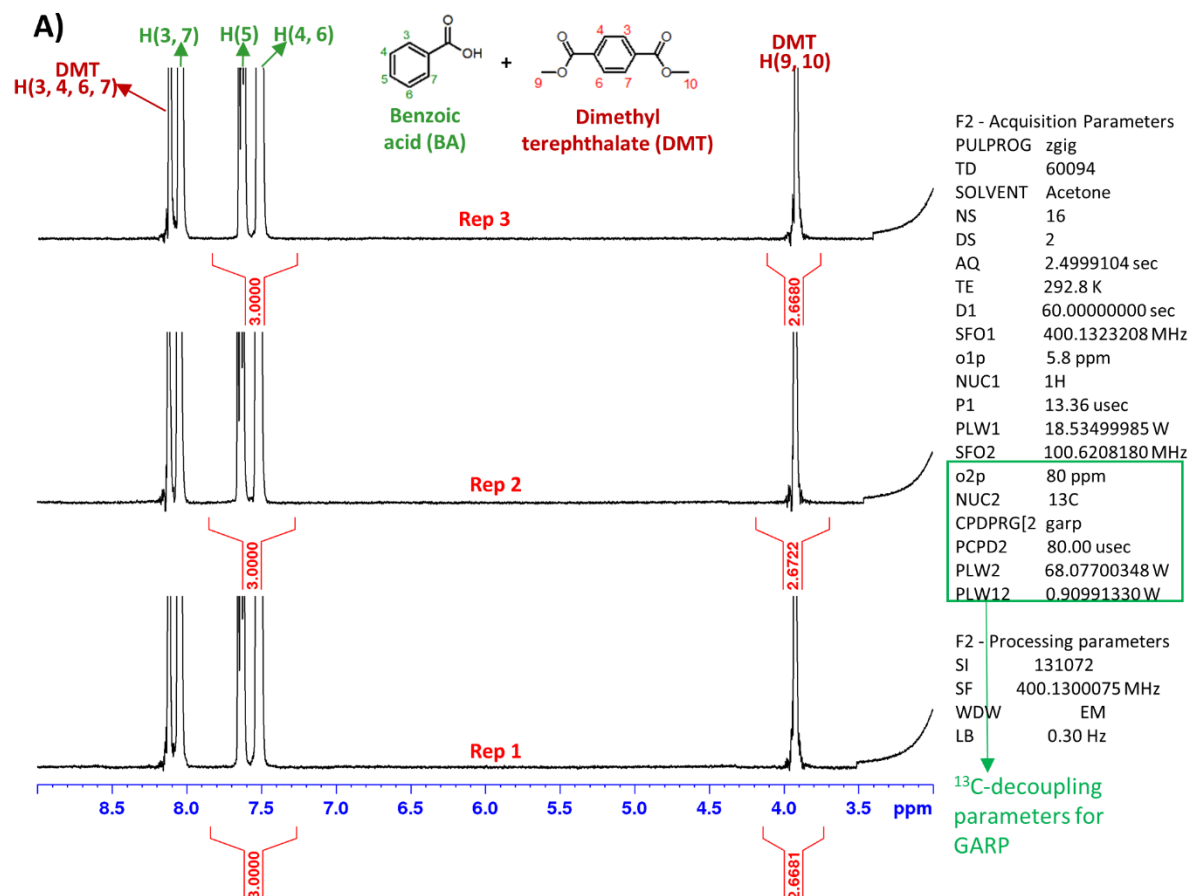


Figure S11. Three replicate $^1\text{H}\{^{13}\text{C}\}$ -qNMR spectra of DMT (analyte) and BA (calibrant) in acetone- d_6 via (A) GARP decoupling and (B) WURST-20 bi-level adiabatic decoupling obtained at 400 MHz. No ^{13}C -satellites were observed if decoupling was performed using the listed acquisition parameters. Please see pg. S25 for purity calculations.

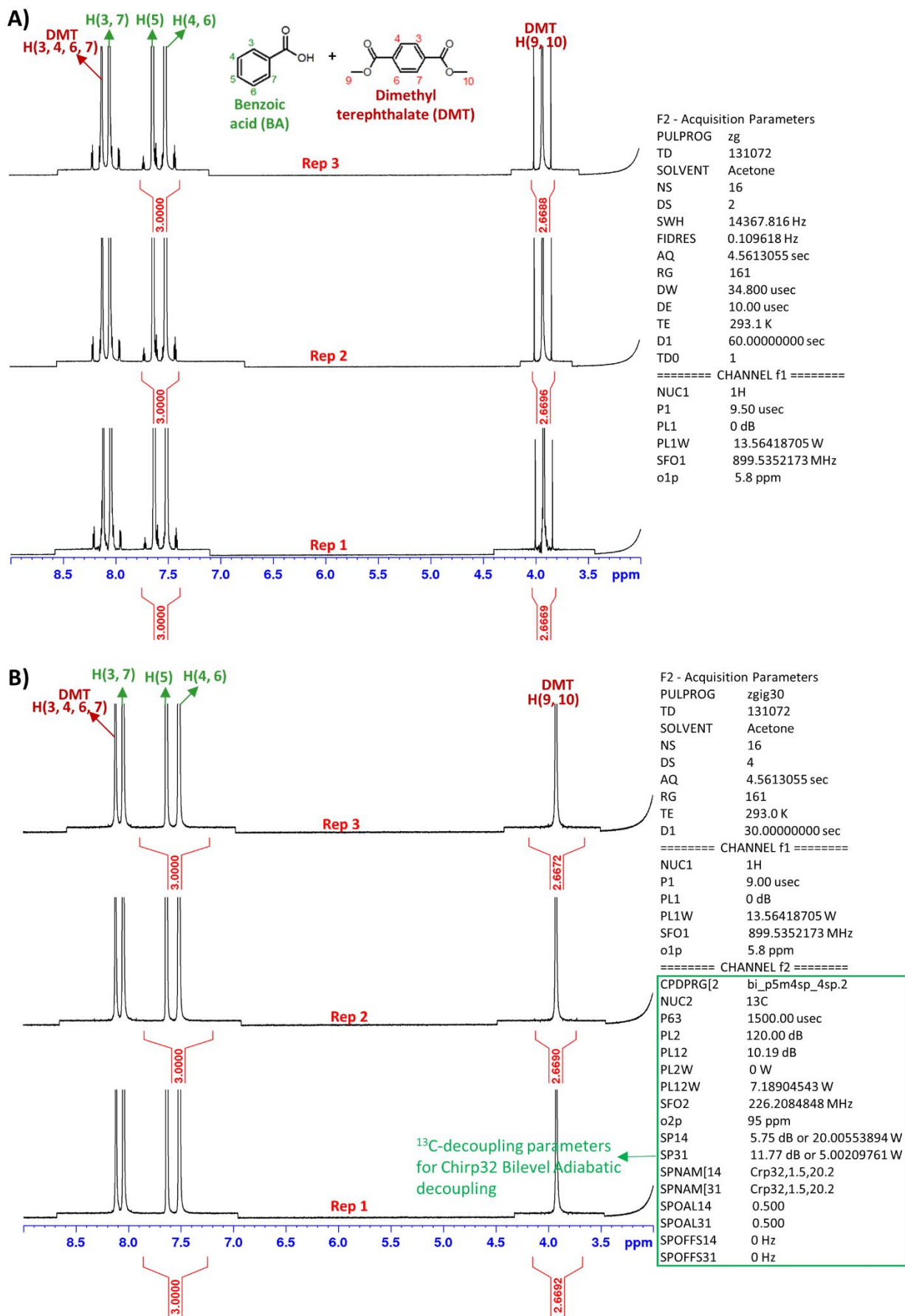


Figure S12. Three replicate ^1H -qNMR and $^1\text{H}\{^{13}\text{C}\}$ -qNMR spectra of DMT (analyte) and BA (internal standard) in acetone- d_6 recorded at 900 MHz. (A) In the ^1H -qNMR spectra, the integral for H(5) + H(4, 6), including its ^{13}C -satellites, was fully resolved from the integral of H(3, 7). (B) Bi-level adiabatic decoupling via Chirp32 according to the listed parameters fully decoupled all ^{13}C -satellites. Please see pg. S26 for purity calculations.

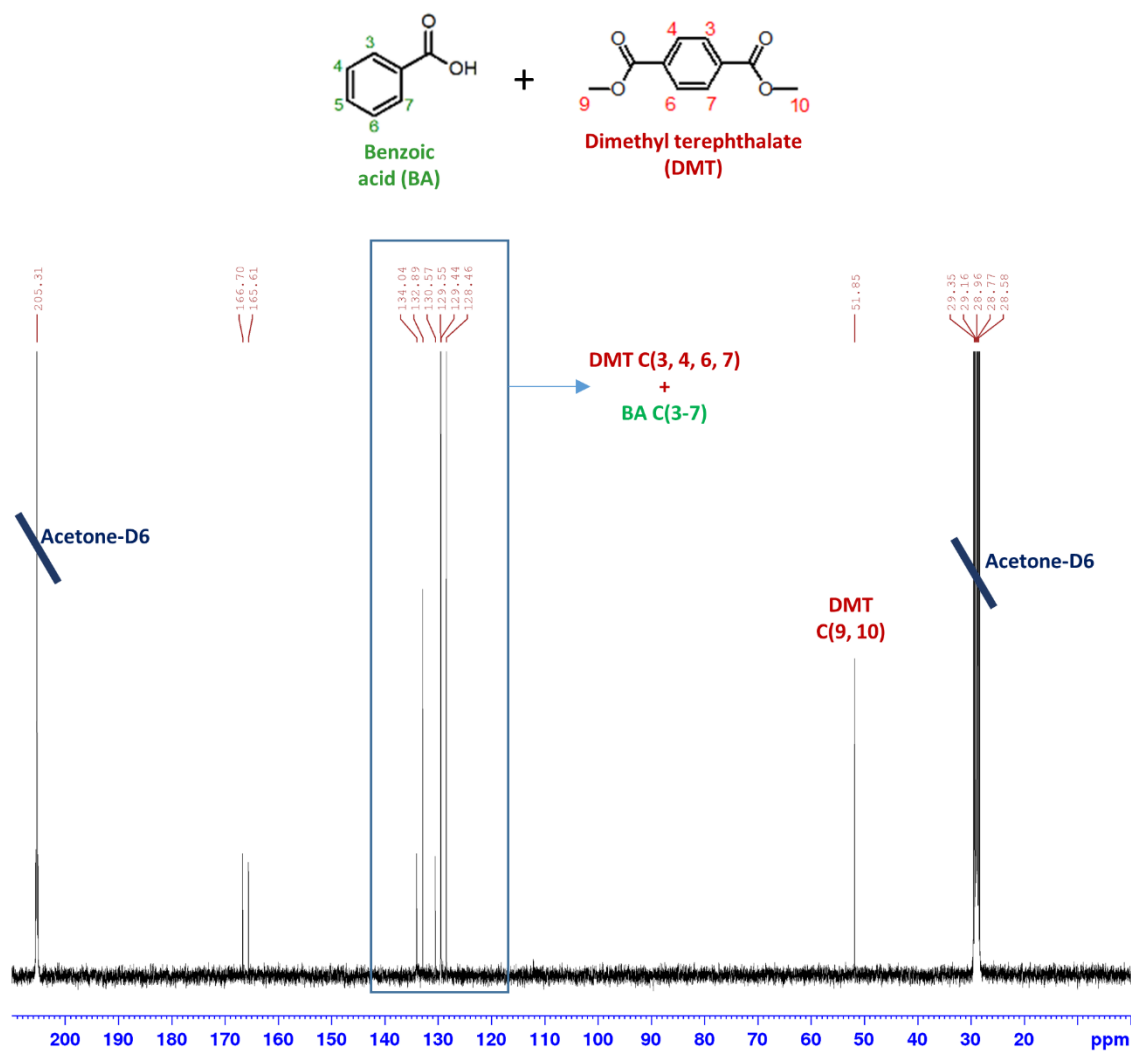


Figure S13. The ^{13}C -spectrum of DMT + BA in acetone-d₆ recorded at 400 MHz. The carbon atoms bonded to protons that need to be decoupled were located in the range 52-134 ppm and centered at around 95 ppm.

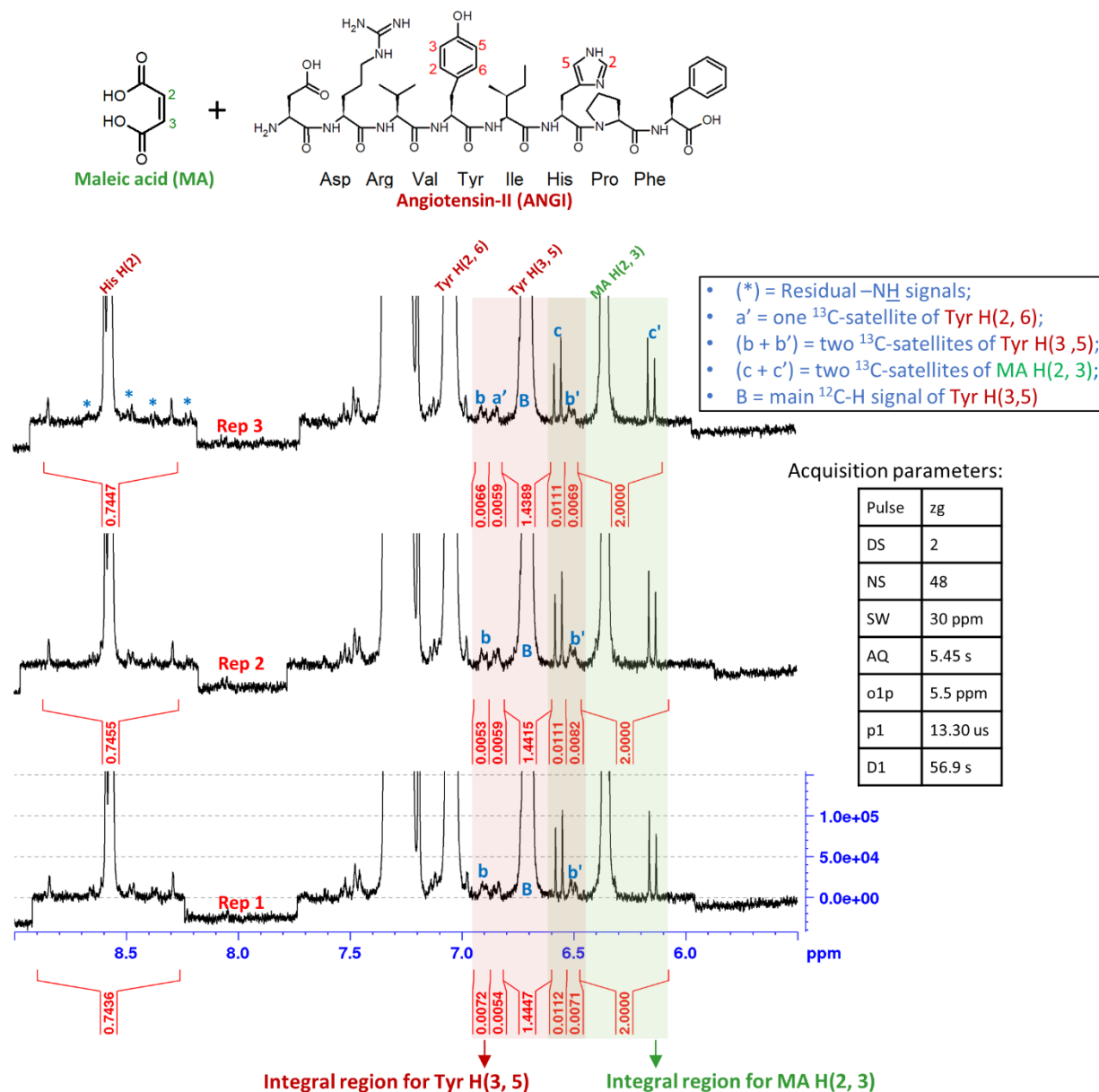


Figure S14. Three replicate ^1H -qNMR spectra of angiotensin-II (analyte) and MA (calibrant) in D_2O recorded at 400 MHz. The longest T_1 at 5.69 s belonged to maleic acid according to an inverse recovery experiment. The integral for His H(2) was discarded because of interference from at least 4 residual -NH signals. Tyr H(3, 5) was the angiotensin-II integral of choice (pink highlight) for purity calculations, but two ^{13}C -satellite interferences were noted: interference from a', one ^{13}C -satellite of Tyr H(2, 6) and interference from c, one ^{13}C -satellite of MA H(2, 3). Concurrently, b', one ^{13}C -satellite of Tyr H(3, 5) interfered with the integral region for MA (green highlight). Necessary adjustments were made to obtain an accurate integral values for MA H(2, 3) and Tyr H(3, 5) (see below). Please see pg. S27 for purity calculations.

The corrected integral for MA H(2, 3) = 2 + c

The corrected integral for Tyr H(3, 5) = B + b + b'

Table S3. The corrected integrals for MA H(2, 3) and Tyr H(3, 5) of angiotensin II.

	Corrected integral for MA H(2, 3)	Corrected integral for Tyr H(3, 5)
Rep 1	2.0112	1.4590
Rep 2	2.0111	1.4550
Rep 3	2.0111	1.4524

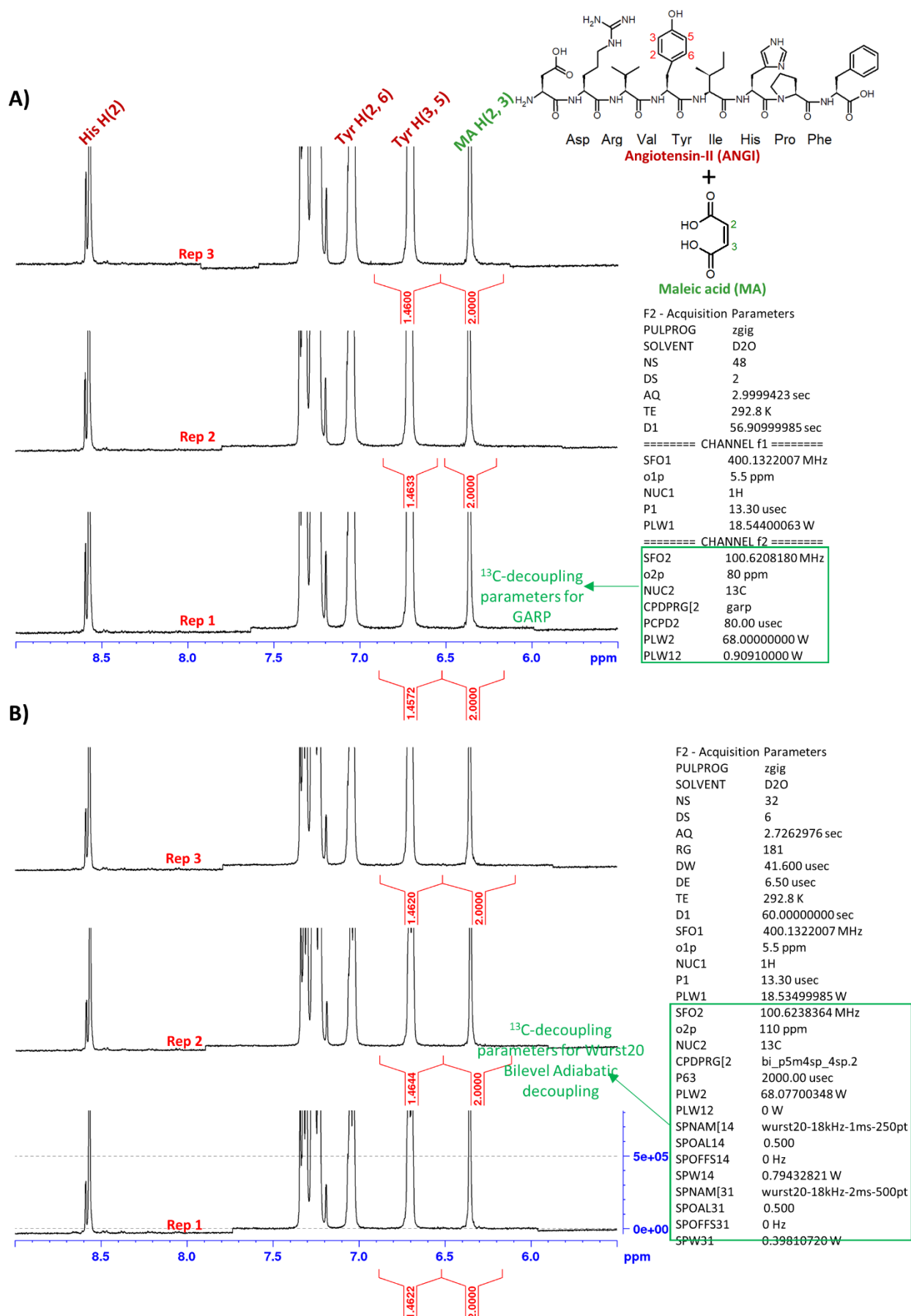


Figure S15. Three replicate $^1\text{H}\{^{13}\text{C}\}$ -qNMR spectra of angiotensin II (analyte) and maleic acid (calibrant) in D_2O via (A) GARP decoupling and (B) WURST-20 bi-level adiabatic decoupling obtained at 400 MHz. No ^{13}C -satellites were observed if decoupling was performed using the listed acquisition parameters. For purity calculations, please see pg. S27.

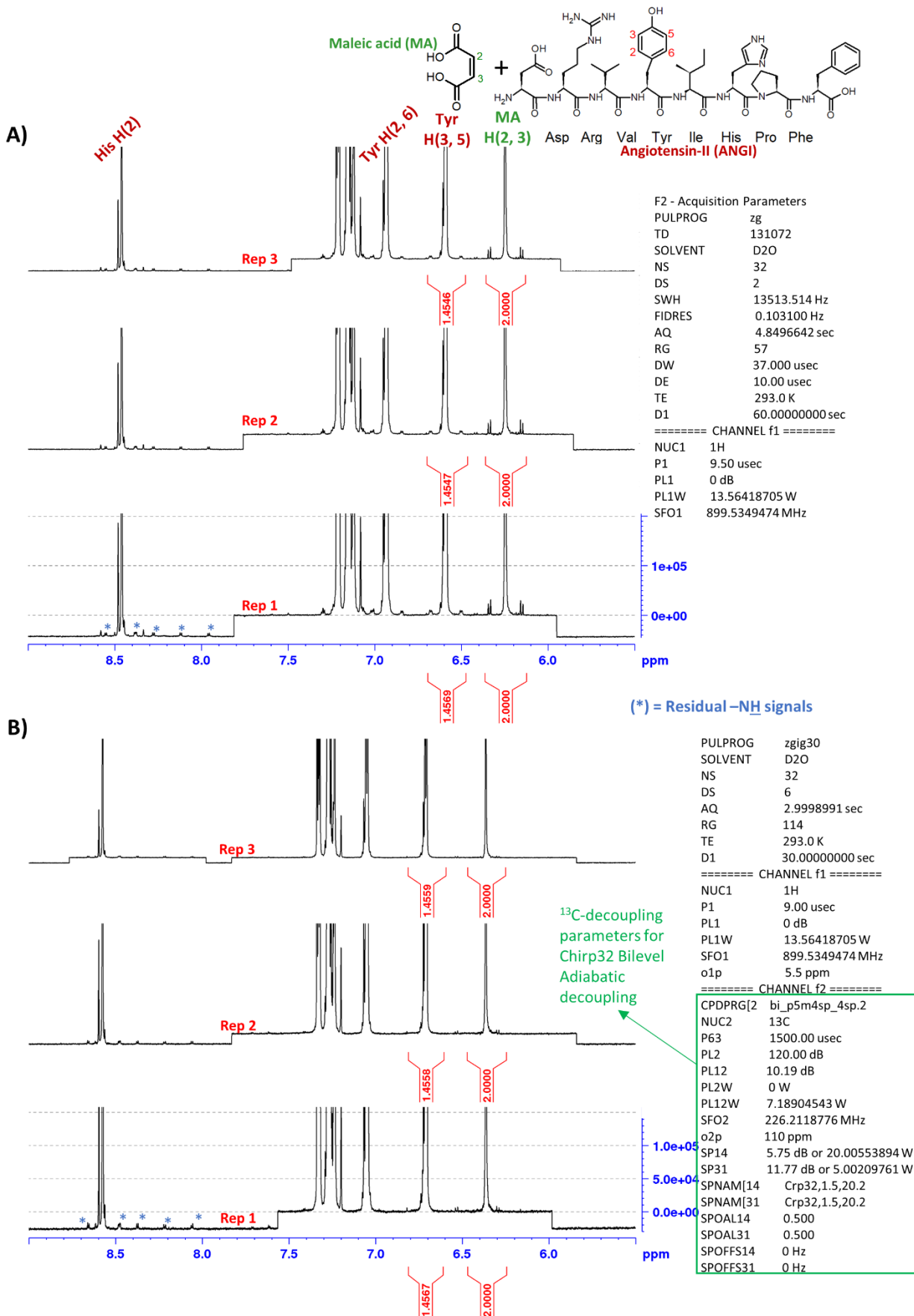


Figure S16. Three replicate ^1H -qNMR and $^1\text{H}\{^{13}\text{C}\}$ -qNMR spectra of angiotensin II (analyte) and maleic acid (calibrant) in D_2O recorded at 900 MHz. Residual -NH integrals interfered with His H(2), which was not integrated. (A) In the ^1H -qNMR spectra, the integral for Tyr H(3, 5), including its ^{13}C -satellites, was fully resolved from the integral of MA H(2, 3). (B) Bi-level adiabatic decoupling via Chirp32 according to the listed parameters fully decoupled all ^{13}C -satellites. For purity calculations, please see pg. S29.

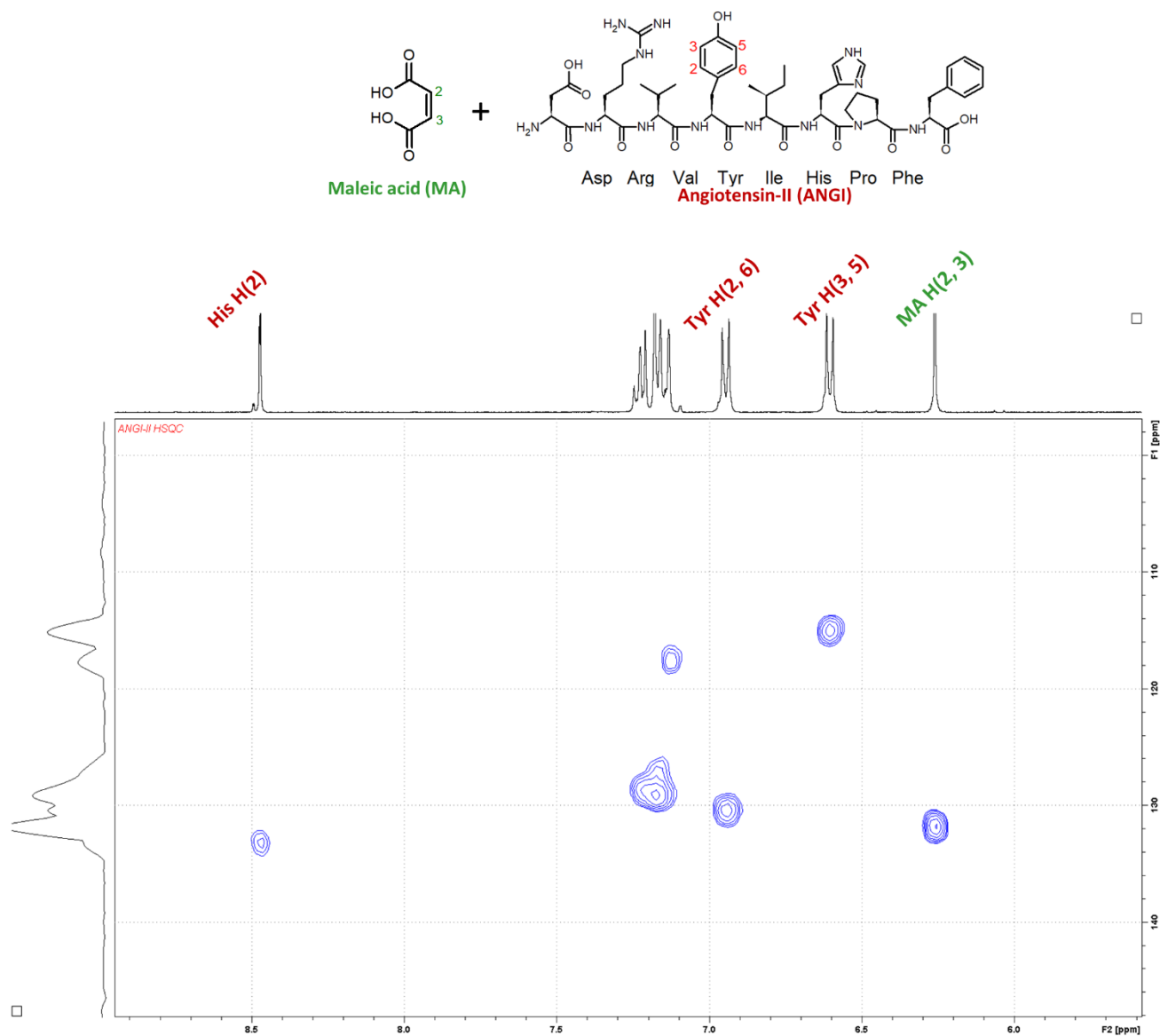


Figure S17. The HSQC spectrum of angiotensin II (analyte) + maleic acid (calibrant) in D_2O recorded at 400 MHz showed that all ^{13}C -atoms for tyrosine and maleic acid are located within 115 to 135 ppm.

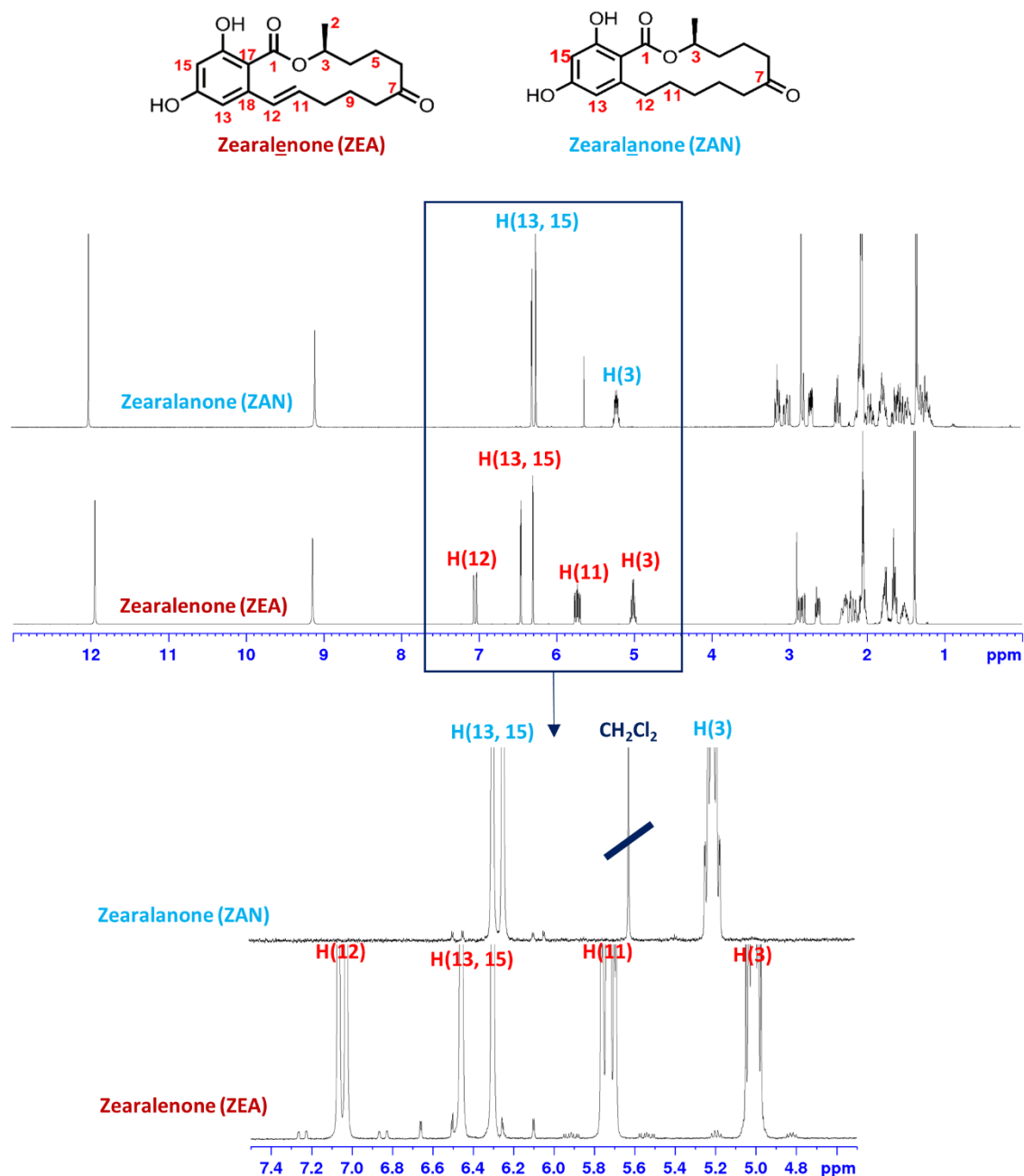


Figure S18. The overlay of the ^1H -NMR spectra of zearalenone (ZEA) over zearalanone (ZAN) showed that the signals for H(13, 15) and H(3) for both compounds overlapped. H(3) of ZAN was potentially concealed by a ^{13}C -satellite of H(3) belonging to ZEA at 5.2 ppm. H(13, 15) of ZAN overlapped with both the main signal and ^{13}C -satellite of H(13, 15) of ZEA.

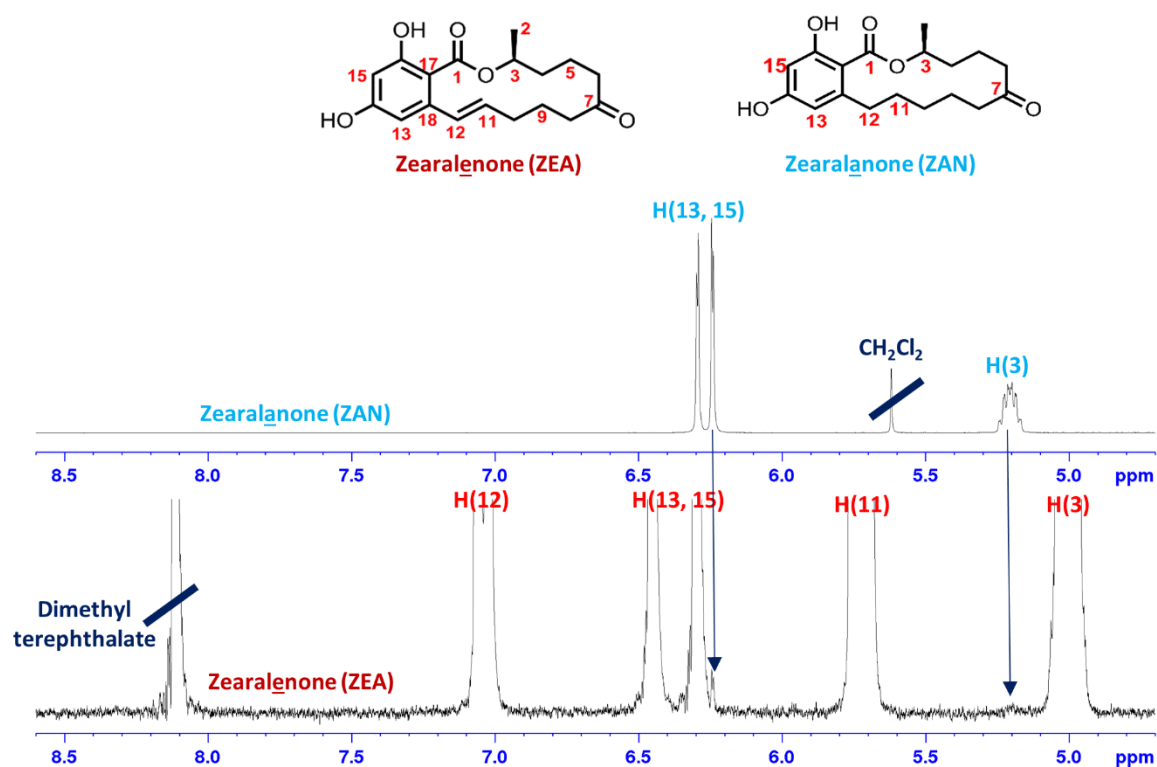


Figure S19. The overlay of the GARP-mediated $^1\text{H}\{^{13}\text{C}\}$ -NMR spectra of zearalenone (ZEA) over zearalanone (ZAN) provided a clear picture of the overlap of the signals for H(13, 15) and H(3) for both compounds. The overlap of H(3) of ZAN with the ^{13}C -satellite of H(3) belonging to ZEA at 5.2 ppm was almost spot on. Part of the H(13, 15) signal of ZAN was clearly observed in the $^1\text{H}\{^{13}\text{C}\}$ -NMR spectra of ZEA. As shown in Supp. Info Fig. S17, this signal was completely concealed by one of the ^{13}C -satellite of H(13, 15) of ZEA in the ^1H -NMR spectra.

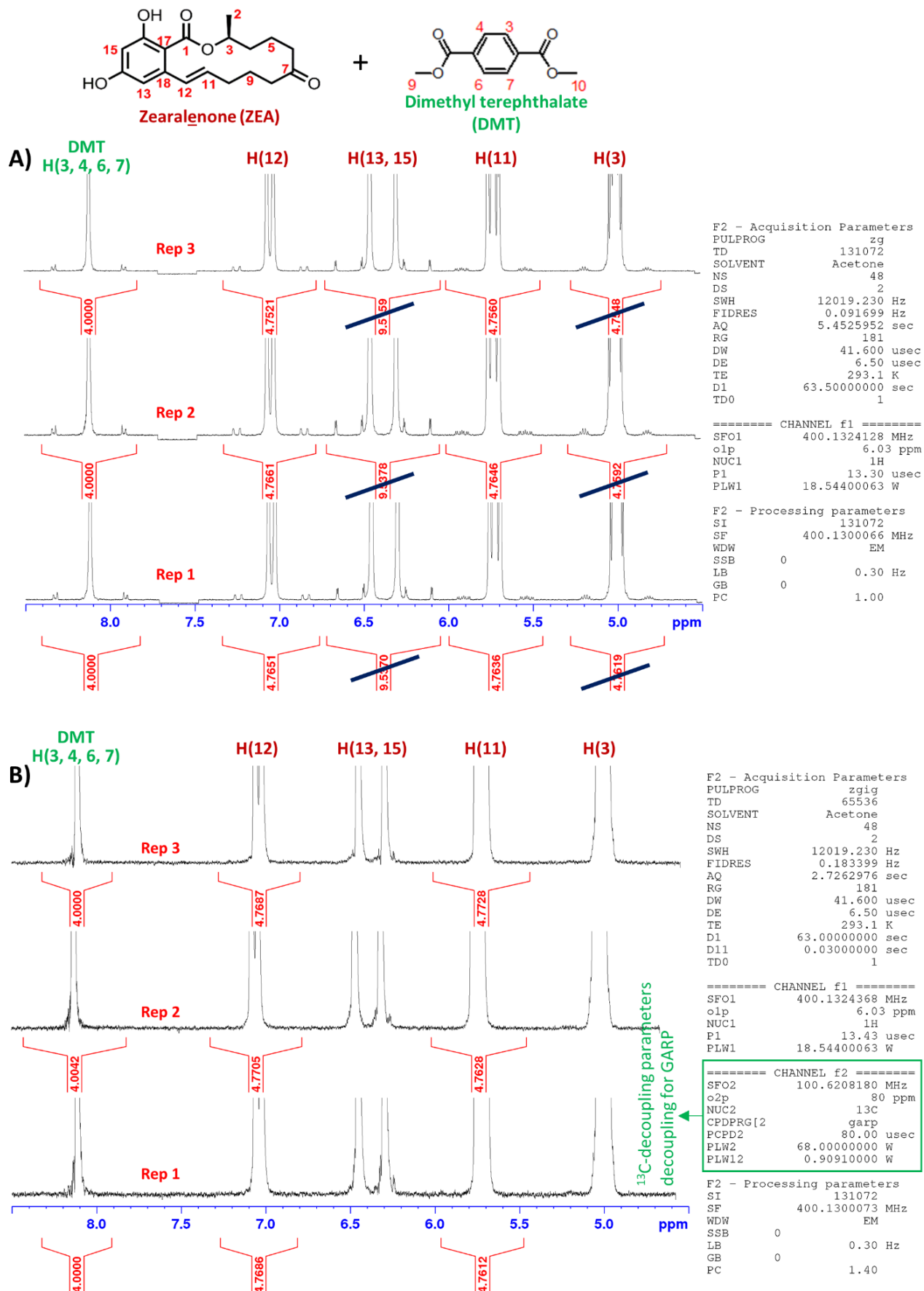


Figure S20. Three replicate ^1H -qNMR (A) and GARP-mediated $^1\text{H}\{^{13}\text{C}\}$ -qNMR (B) spectra of zearalenone (analyte) and dimethyl terephthalate (calibrant) in acetone- D_6 recorded at 400 MHz are depicted. For both ^1H -qNMR and $^1\text{H}\{^{13}\text{C}\}$ -qNMR spectra, the signals for H(12) and H(11) of zearalenone were the only ones integrated for purity calculations (see Supp. Info page S30).

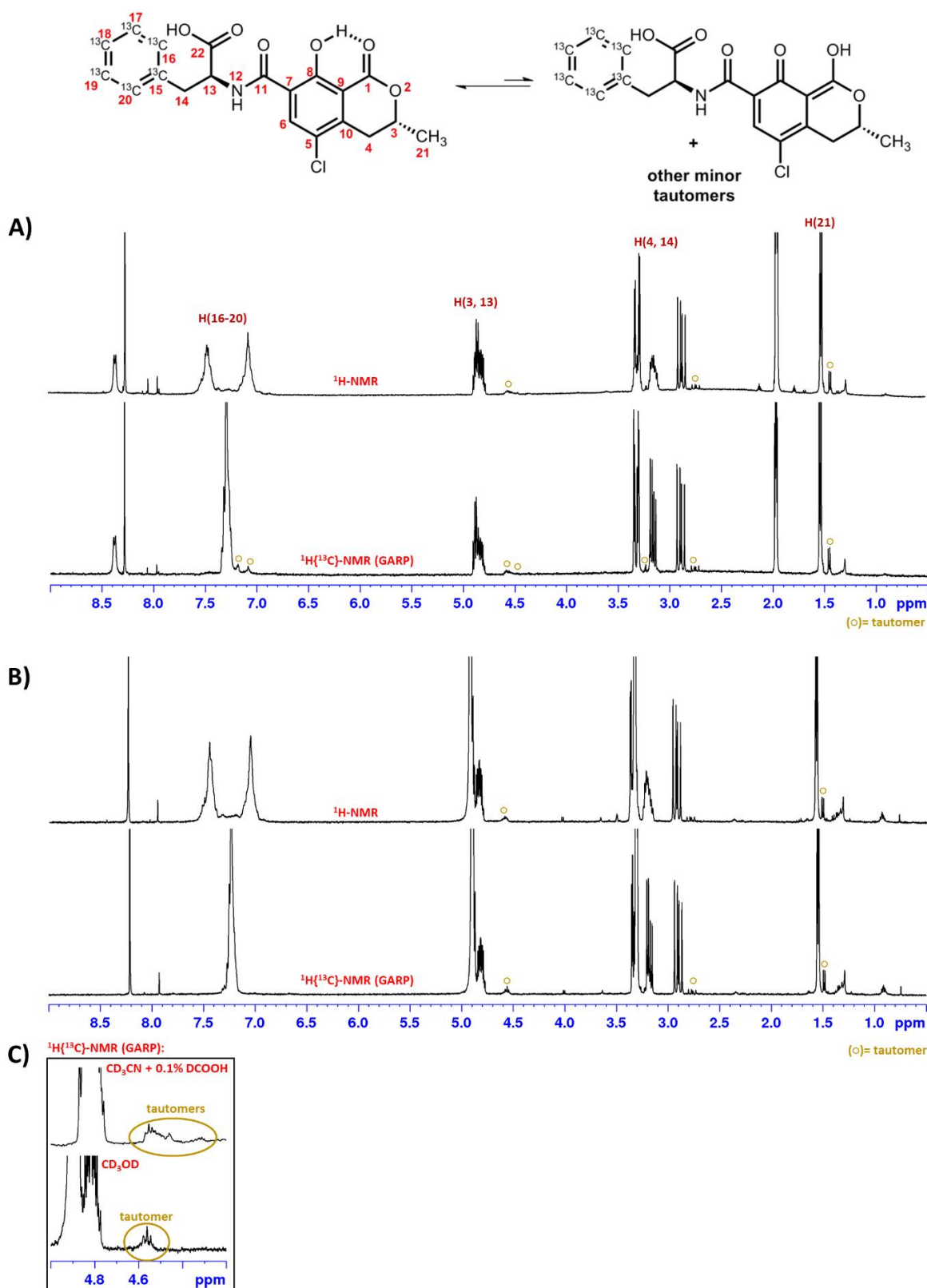


Figure S21. The ^1H -NMR and GARP-mediated $^1\text{H}\{^{13}\text{C}\}$ -NMR spectra of $^{13}\text{C}_6$ -ochratoxin A in $\text{CD}_3\text{CN} + 0.1\% \text{DCOOH}$ and CD_3OD respectively. **(A)** The positions of most of the tautomers were identified with more clarity from the $^1\text{H}\{^{13}\text{C}\}$ -NMR spectrum recorded in $\text{CD}_3\text{CN} + 0.1\% \text{DCOOH}$ than from the ^1H -NMR spectrum. **(B)** When the NMR solvent was switched to CD_3OD , fewer tautomers were produced. As a polar hydrogen bonding solvent, CD_3OD has the ability to disturb intramolecular hydrogen bonding patterns that leads to the formation of tautomers. However, the intramolecular hydrogen bond in the coumarin portion of ochratoxin A appeared to be quite stable, such that its enol tautomer (depicted in the equation above) likely remained, even in the presence of CD_3OD . **(C)** A close-up look at the $\text{H}(3, 13)$ peak clearly showed that at the most, only one tautomer appeared in CD_3OD , while several were detected in $\text{CD}_3\text{CN} + 0.1\% \text{DCOOH}$. This tautomer was suspected to adopt the enol conformation.

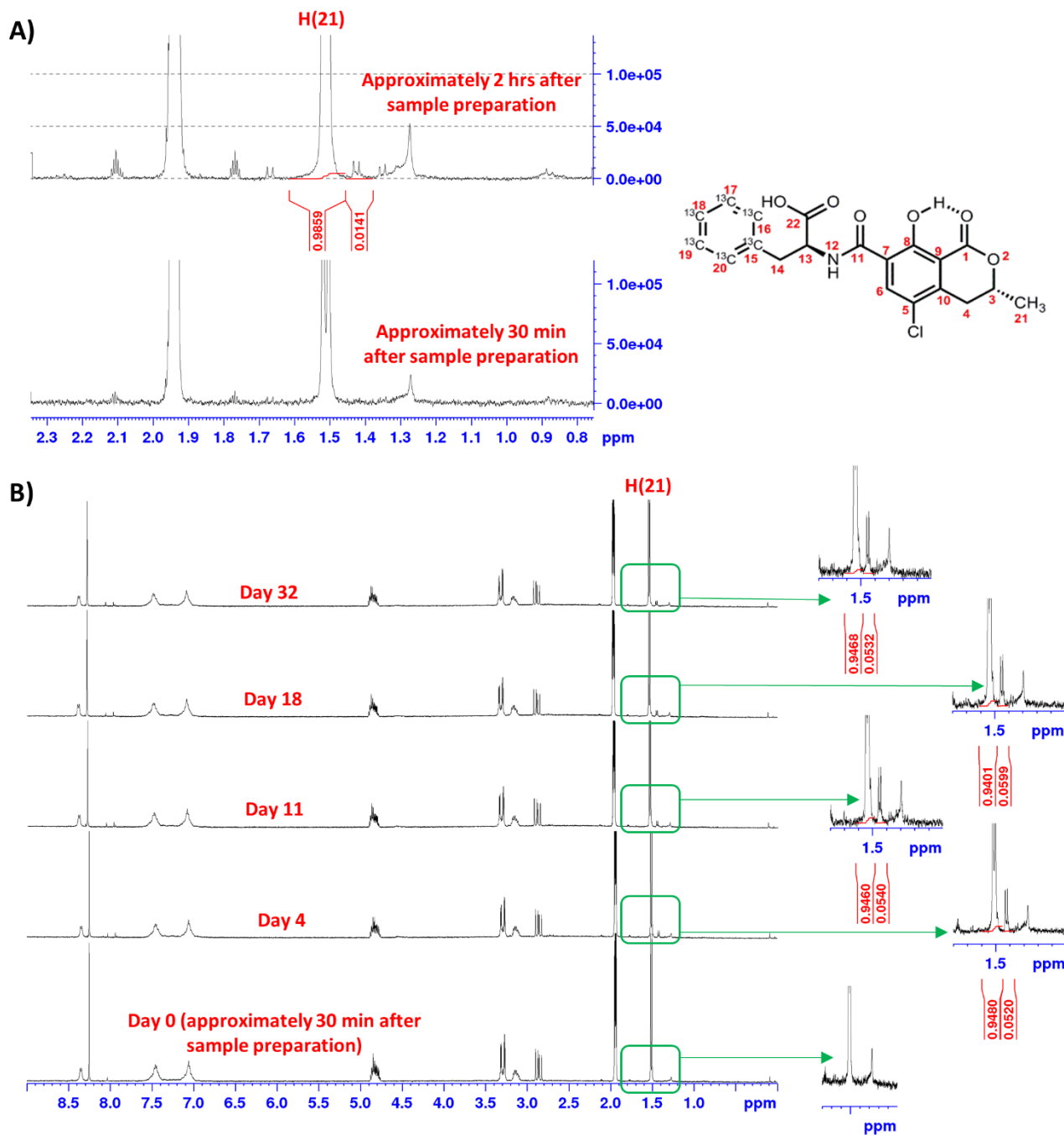


Figure S22. Monitoring the doublet for the methyl group at position 21 for signs of tautomerization when $^{13}\text{C}_6$ -ochratoxin A was dissolved in $\text{CD}_3\text{CN} + 0.1\% \text{ DCOOH}$. **(A)** No tautomers were observed from a freshly prepared sample. However, within 2 hours a tautomer peak emerged at about 1.4 % of the main signal. **(B)** The sample was continuously monitored over several days/weeks. On day 4, tautomerization had stabilized at about 5-6% and remained as such up to 32 days post sample preparation. No degradation occurred, confirming that tautomerization did not lead to decomposition of $^{13}\text{C}_6$ -ochratoxin A.

NOTE: The sample was stored at -20°C , when not in use for NMR analysis.

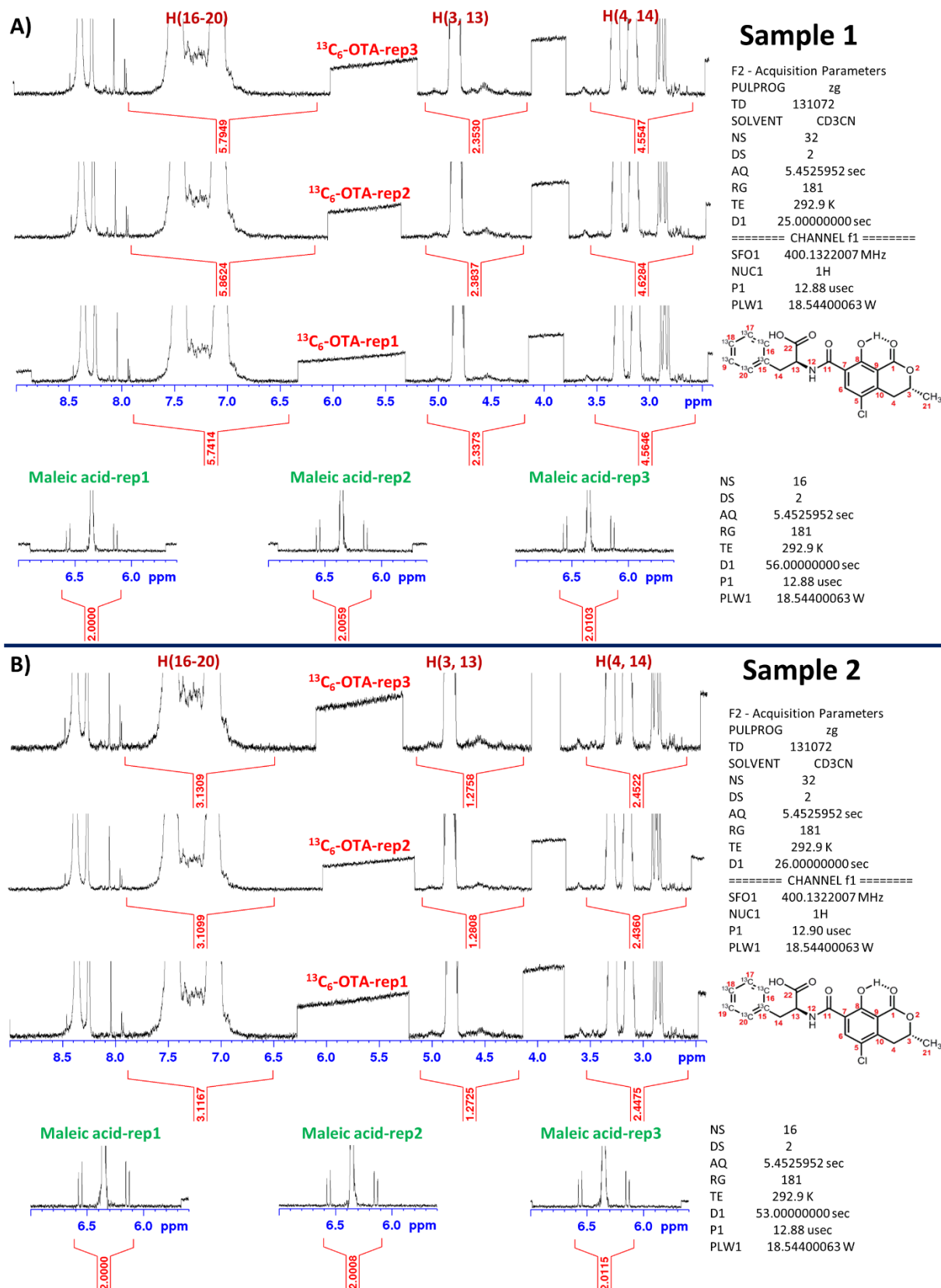


Figure S23. The concentration of ¹³C₆-ochratoxin A in samples 1(A) and 2 (B) was determined by ¹H-qNMR with maleic acid as the external standard in CD₃CN + 0.1% DCOOH as the solvent. Each maleic acid and ¹³C₆-ochratoxin A sample pair was prepared fresh and analyzed on the same day. Three replicate spectra were recorded. For integration purposes, the integral of maleic acid from the first replicate spectrum was set to 2.0000. The integration for all subsequent replicates for maleic acid and ¹³C₆-ochratoxin A, were adjusted to the same scale as the integration maleic acid in replicate 1. This was achieved by using the Topspin command “use lastscale for calibration” when integrating. The final concentration of ¹³C₆-ochratoxin A in each sample was calculated as shown on pg. S34 (Sample 1) and pg. S36 (Sample 2).

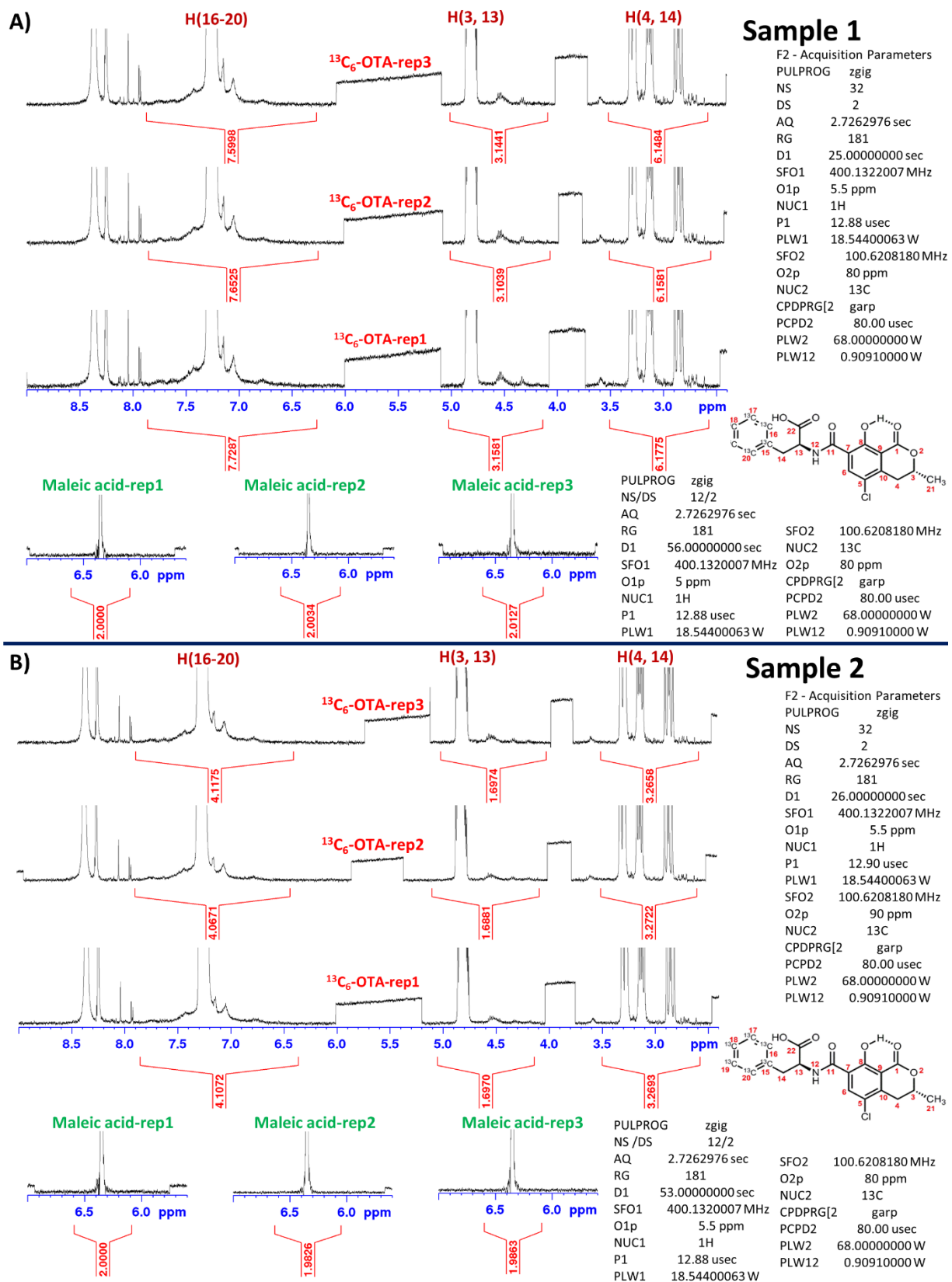


Figure S24. The concentration of $^{13}\text{C}_6$ -ochratoxin A in samples 1(A) and 2 (B) was determined by GARP-mediated $^1\text{H}\{^{13}\text{C}\}$ -qNMR with maleic acid as the external standard in $\text{CD}_3\text{CN} + 0.1\% \text{DCOOH}$ as the solvent. Each maleic acid and $^{13}\text{C}_6$ -ochratoxin A sample pair was prepared fresh and analyzed on the same day in triplicates. For integration purposes, the integral of maleic acid from the first replicate spectrum was set to 2.0000. The integration for all subsequent replicates for maleic acid and $^{13}\text{C}_6$ -ochratoxin A, were adjusted to the same scale as the integration maleic acid in replicate 1. This was achieved by using the Topspin command “use lastscale for calibration” when integrating. The final concentration of $^{13}\text{C}_6$ -ochratoxin A in each sample was calculated as shown on pg. S34 (Sample 1) and pg. S36 (Sample 2).

Table S1. The % standard deviation of integral replicates for dimethyl terephthalate, zearalenone and ¹³C₆-ochratoxin A.

	DMT^a	Zearalenone		¹³C₆-ochratoxin A-Sample 1		
	H(9, 10)	H(12)	H(11)	H(16-20)	H(3, 13)	H(4, 14)
Replicate 1	2.6616	4.7651	0.9895	5.7414	2.3373	4.5646
Replicate 2	2.6585	4.7661	0.9897	5.8624	2.3837	4.6284
Replicate 3	2.6584	4.7521	0.9879	5.7949	2.3530	4.5547
SD	0.001819	0.007810	0.000987	0.060635	0.023601	0.040000
RSD (%)	0.2	0.8	0.1	6.1	2.4	4.0

^aDMT = dimethyl terephthalate

NOTE: all integrals were recorded from ¹H-qNMR at 400 MHz and are lifted from pg. S25 for dimethyl terephthalate, pg. S30 for zearalenone and pg. S31 for ¹³C₆-ochratoxin A (sample 1). These integrals were chosen because they did not require a correction.

The purity of dimethyl terephthalate (analyte) with benzoic acid PS1 (internal standard) at 400 and 900 MHz

Purity equation for quantitative NMR with an internal standard:

$$w_{an} = \frac{I_{an}}{I_c} \cdot \frac{N_c}{N_{an}} \cdot \frac{MW_{an}}{MW_c} \cdot \frac{m_c}{m_{an}} \cdot \frac{V_{an}}{V_c} \cdot w_c$$

Where

I_{an} = integral of analyte

N_{an} = number of ^1H nuclei giving rise to integral of the analyte = 6 for DMT H(9, 10)

MW_{an} = molecular weight of analyte = 194.185 g/mol

m_{an} = mass of analyte = 14.9457 mg

V_{an} = volume of analyte

w_{an} = purity of analyte

I_c = integral of calibrant

N_c = number of ^1H nuclei giving rise to integral of the calibrant = 3

MW_c = molecular weight of standard = 122.122 g/mol

m_c = mass of standard = 21.1197 mg

V_c = volume of standard

w_c = purity of standard = 999.92 mg/g

For quantitation using an internal standard, the analyte and standard are in the same sample. Therefore $V_{an} = V_c$ and cancel each other.

The qHNMR purity of dimethyl terephthalate at 400 MHz:

	I_c	I_{an}	^1H -qNMR purity (g/g)
Replicate 1	2.9890	2.6616	1.0003
Replicate 2	2.9885	2.6585	0.9993
Replicate 3	2.9885	2.6584	0.9993
Average			0.9997
SD			0.0007

The qH $\{^{13}\text{C}\}$ NMR purity of dimethyl terephthalate at 400 MHz via GARP decoupling:

	I_c	I_{an}	$^1\text{H}\{^{13}\text{C}\}$ -qNMR purity (g/g)
Replicate 1	3.0000	2.6681	0.9991
Replicate 2	3.0000	2.6722	1.0006
Replicate 3	3.0000	2.6680	0.9991
Average			0.9996
SD			0.0011

The qH $\{^{13}\text{C}\}$ NMR purity of dimethyl terephthalate at 400 MHz via WURST-20 bi-level adiabatic decoupling:

	I_c	I_{an}	$^1\text{H}\{^{13}\text{C}\}$ -qNMR purity (g/g)
Replicate 1	3.0000	2.6683	0.9992
Replicate 2	3.0000	2.6705	1.0000
Replicate 3	3.0000	2.6669	0.9987
Average			0.9993
SD			0.0008

The qHNMR purity of dimethyl terephthalate at 900 MHz:

	I_c	I_{an}	^1H -qNMR purity (g/g)
Replicate 1	3.0000	2.6669	0.9987
Replicate 2	3.0000	2.6696	0.9997
Replicate 3	3.0000	2.6688	0.9994
Average			0.9992
SD			0.0006

The qH{ ^{13}C }NMR purity of dimethyl terephthalate at 900 MHz via Chirp-32 bi-level adiabatic decoupling:

	I_c	I_{an}	$^1\text{H}\{^{13}\text{C}\}$ -qNMR purity (g/g)
Replicate 1	3.0000	2.6672	0.9988
Replicate 2	3.0000	2.6690	0.9994
Replicate 3	3.0000	2.6669	0.9987
Average			0.9990
SD			0.0005

The ANOVA: Single factor comparison between ^1H , GARP and bi-level adiabatic decoupling qNMR results recorded at 400 MHz:

SUMMARY

Groups	Count	Sum	Average	Variance
Proton	3	2.998961451	0.999653817	3.38148E-07
GARP	3	2.998800635	0.999600212	8.05339E-07
Bilevel Adiabatic	3	2.997827035	0.999275678	4.61796E-07

ANOVA

Source of Variation	SS	df	MS	F	P-value	F crit
Between groups	2.51E-07	2	1.25592E-07	0.234710301	0.797733058	5.14325285
Within groups	3.21E-06	6	5.35094E-07			
Total	3.46E-06	8				

The ANOVA: Single factor comparison between ^1H and bi-level adiabatic decoupling qNMR results for data recorded at 900 MHz:

SUMMARY

Groups	Count	Sum	Average	Variance
Proton	3	2.99767725	0.99922575	2.69693E-07
Bilevel Adiabatic	3	2.996853435	0.998951145	1.80886E-07

ANOVA

Source of Variation	SS	df	MS	F	P-value	F crit
Between groups	1.13E-07	1	1.13112E-07	0.502074689	0.517700208	7.708647422
Within groups	9.01E-07	4	2.25289E-07			
Total	1.01E-06	5				

The purity of angiotensin-II (analyte) with maleic acid (internal standard) at 400 MHz

Purity equation for quantitative NMR with an internal standard:

$$w_{an} = \frac{I_{an}}{I_c} \cdot \frac{N_c}{N_{an}} \cdot \frac{MW_{an}}{MW_c} \cdot \frac{m_c}{m_{an}} \cdot \frac{V_{an}}{V_c} \cdot w_c$$

Where

I_{an} = integral of analyte

N_{an} = number of ^1H nuclei giving rise to integral of the analyte = 2 for Tyr H(3, 5)

MW_{an} = molecular weight of analyte = 1046.1890 g/mol

m_{an} = mass of analyte = 10.8001 mg

V_{an} = volume of analyte

w_{an} = purity of analyte

I_c = integral of standard

N_c = number of ^1H nuclei giving rise to integral of the calibrant = 2

MW_c = molecular weight of standard = 116.0722 g/mol

m_c = mass of standard = 1.1597 mg

V_c = volume of standard

w_c = purity of standard = 998.9 mg/g

For quantitation using an internal standard, the analyte and standard are in the same sample. Therefore $V_{an} = V_c$ and cancel each other.

The qHNMR purity of angiotensin II at 400 MHz:

	I_c	I_{an}	^1H -qNMR purity (g/g)
Replicate 1	2.0112	1.4590	0.7013
Replicate 2	2.0111	1.4550	0.6994
Replicate 3	2.0111	1.4524	0.6982
Average			0.6997
SD			0.0019

The qH $\{^{13}\text{C}\}$ NMR purity of angiotensin II at 400 MHz via GARP decoupling:

	I_c	I_{an}	$^1\text{H}\{^{13}\text{C}\}$ -qNMR purity (g/g)
Replicate 1	2.0000	1.4572	0.7044
Replicate 2	2.0000	1.4633	0.7073
Replicate 3	2.0000	1.4600	0.7057
Average			0.7058
SD			0.0018

The qH $\{^{13}\text{C}\}$ NMR purity of angiotensin II at 400 MHz via WURST-20 bi-level adiabatic decoupling:

	I_c	I_{an}	$^1\text{H}\{^{13}\text{C}\}$ -qNMR purity (g/g)
Replicate 1	2.0000	1.4622	0.7068
Replicate 2	2.0000	1.4644	0.7079
Replicate 3	2.0000	1.4622	0.7068
Average			0.7072
SD			0.0007

The ANOVA: Single factor comparison between ¹H, GARP and bi-level adiabatic decoupling results obtained at 400 MHz:

SUMMARY				
<i>Groups</i>	<i>Count</i>	<i>Sum</i>	<i>Average</i>	<i>Variance</i>
Proton	3	2.098977	0.699658931	2.5E-06
GARP	3	2.117477	0.705825646	2.18E-06
Bilevel Adiabatic	3	2.121489	0.707163017	3.77E-07

ANOVA						
<i>Source of Variation</i>	<i>SS</i>	<i>df</i>	<i>MS</i>	<i>F</i>	<i>P-value</i>	<i>F crit</i>
Between groups	9.61E-05	2	4.80641E-05	28.54734	0.00086	5.143253
Within groups	1.01E-05	6	1.68366E-06			
Total	0.000106	8				

The ANOVA comparison above showed that statistically different results is obtained when comparing angiotensin II purity values obtained from qHNMR, GARP and bi-level adiabatic decoupling data.

The ANOVA: Single factor comparison between GARP and bi-level adiabatic decoupling data recorded at 400 MHz:

SUMMARY GARP/BAD 400 MHz				
<i>Groups</i>	<i>Count</i>	<i>Sum</i>	<i>Average</i>	<i>Variance</i>
GARP	3	2.117477	0.705826	2.18E-06
Bilevel Adiabatic	3	2.121489	0.707163	3.77E-07

ANOVA						
<i>Source of Variation</i>	<i>SS</i>	<i>df</i>	<i>MS</i>	<i>F</i>	<i>P-value</i>	<i>F crit</i>
Between groups	2.68E-06	1	2.68E-06	2.099665	0.220918	7.708647
Within groups	5.11E-06	4	1.28E-06			
Total	7.79E-06	5				

As shown above, when only GARP and bi-level adiabatic decoupling angiotensin II purity values are compared by ANOVA, the results are statistically equivalent. This comparison suggested that the qHNMR data stood out as different. Individual ANOVA comparing the results of qHNMR vs GARP only and qHNMR vs bi-level adiabatic decoupling only, confirmed that the qHNMR purity value for angiotensin II stands out as statistically different (data not shown).

The purity of angiotensin-II (analyte) with maleic acid (internal standard) at 900 MHz

The qHNMR purity value of angiotensin II at 900 MHz:

	I_c	I_{an}	^1H -qNMR purity (g/g)
Replicate 1	2.0000	1.4569	0.7042
Replicate 2	2.0000	1.4547	0.7032
Replicate 3	2.0000	1.4546	0.7031
Average			0.7035
SD			0.0008

The qH $\{^{13}\text{C}\}$ NMR purity value of angiotensin II at 900 MHz via Chirp-32 bi-level adiabatic decoupling:

	I_c	I_{an}	$^1\text{H}\{^{13}\text{C}\}$ -qNMR purity (g/g)
Replicate 1	2.0000	1.4567	0.7041
Replicate 2	2.0000	1.4558	0.7037
Replicate 3	2.0000	1.4559	0.7038
Average			0.7039
SD			0.0003

The ANOVA: Single factor comparison between qHNMR and bi-level adiabatic decoupling data for angiotensin II recorded at 900 MHz:

SUMMARY

Groups	Count	Sum	Average	Groups
Proton	3	2.110565	0.703521501	3.95E-07
Bilevel Adiabatic	3	2.111628	0.703875985	5.69E-08

ANOVA

Source of Variation	SS	df	MS	F	P-value	F crit
Between groups	1.88E-07	1	1.88488E-07	0.834483	0.41266	7.708647
Within groups	9.03E-07	4	2.25874E-07			
Total	1.09E-06	5				

The purity of zearalenone (analyte) with dimethyl terephthalate (internal standard) at 400 MHz

Purity equation for quantitative NMR:

$$w_{an} = \frac{I_{an}}{I_c} \cdot \frac{N_c}{N_{an}} \cdot \frac{MW_{an}}{MW_c} \cdot \frac{m_c}{m_{an}} \cdot \frac{V_{an}}{V_c} \cdot w_c$$

Where

I_{an} = integral of analyte

N_{an} = number of ^1H nuclei giving rise to integral of the analyte = 1 for both H(12) and H(11)

MW_{an} = molecular weight of analyte = 318.367 g/mol

m_{an} = mass of analyte = 15.3012 mg

V_{an} = volume of analyte

w_{an} = purity of analyte

I_c = integral of standard

N_c = number of ^1H nuclei giving rise to integral of the standard = 4

MW_c = molecular weight of standard = 194.185 g/mol

m_c = mass of standard = 1.9397 mg

V_c = volume of standard

w_c = purity of standard = 999.4 mg/g

For quantitation using an internal standard, the analyte and calibrant are in the same sample. Therefore $V_{an} = V_c$ and cancel each other.

The qHNMR purity of zearalenone at 400 MHz:

	I_c	I_{an} (H12)	purity from H(12) (g/g)	I_{an} (H11)	purity from H(11) (g/g)	Overall purity (g/g)
Replicate 1	4.0000	4.7651	0.9898	4.7636	0.9895	0.9896
Replicate 2	4.0000	4.7661	0.9900	4.7646	0.9897	0.9898
Replicate 3	4.0000	4.7521	0.9871	4.7560	0.9879	0.9875
Average purity = 0.9890 g/g						
SD = 0.0013 g/g						

The qH $\{^{13}\text{C}\}$ NMR purity of zearalenone at 400 MHz via GARP decoupling:

	I_c	I_{an} (H12)	purity from H(12) (g/g)	I_{an} (H11)	purity from H(11) (g/g)	Overall purity (g/g)
Replicate 1	4.0000	4.7686	0.9905	4.7612	0.9890	0.9897
Replicate 2	4.0000	4.7705	0.9909	4.7628	0.9893	0.9901
Replicate 3	4.0000	4.7687	0.9905	4.7728	0.9914	0.9909
Average purity = 0.9903 g/g						
SD = 0.0006 g/g						

The ANOVA: Single factor comparison between qHNMR and GARP decoupling data for zearalenone

SUMMARY

Groups	Count	Sum	Average	Variance
Proton	3	2.966924903	0.988975	1.69E-06
GARP	3	2.970777985	0.990259	3.89E-07

ANOVA

Source of Variation	SS	df	MS	F	P-value	F crit
Between groups	2.47E-06	1	2.47E-06	2.382363	0.19758662	7.708647
Within groups	4.15E-06	4	1.04E-06			
Total	6.63E-06	5				

The concentration of $^{13}\text{C}_6$ -ochratoxin A (analyte) with maleic acid as external standard for Sample 1

Equation for calculating concentration (g/g) by quantitative NMR with an external standard:

$$[\text{analyte}] = \frac{I_{an}}{I_c} \cdot \frac{N_c}{N_{an}} \cdot \frac{\theta_{an}^{360}}{\theta_c^{360}} \cdot \frac{NS_c}{NS_{an}} \cdot \frac{MW_{an}}{MW_c} \cdot \frac{m_c}{m_c^{soln}} \cdot w_c \text{ in g/g}$$

Where

I_{an} = integral of analyte

N_{an} = number of ^1H nuclei giving rise to integral of the analyte = 5 for H(16-20); 2 for H(3, 13); 4 for H(4, 14)

MW_{an} = molecular weight of analyte = 409.7 g/mol

NS_{an} = number of scans for analyte = 32

θ_{an}^{360} = 360° pulse for analyte = 51.5 μs

I_c = integral of standard

N_c = number of ^1H nuclei giving rise to integral of the standard = 2

MW_c = molecular weight of standard = 116.073 g/mol

m_c = mass of standard = 2.455 mg

NS_c = number of scans for standard = 16 for ^1H -qNMR and 12 for $^1\text{H}\{^{13}\text{C}\}$ -qNMR

θ_c^{360} = 360° pulse for standard = 51.5 μs

m_c^{soln} = mass of standard solution = 1215.985 mg

w_c = purity of standard = 0.9989 g/g

No receiver gain correction was necessary as an RG of 181 was used for both analyte and standard.

The qHNMR concentration of $^{13}\text{C}_6$ -ochratoxin A in Sample 1 at 400 MHz:

Mean I_c = (2.0000+2.0059+2.0103)/3 = 2.0054 (the mean I_c from the three replicates was used for all calculations)

	I_{an}			Concentration (g/g)			Overall concentrations (g/g)
	H(16-20)	H(3, 13)	H(4, 14)	H(16-20)	H(3, 13)	H(4, 14)	
Replicate 1	5.7414	2.3373	4.5646	0.004076	0.004148	0.004051	0.004092
Replicate 2	5.8624	2.3837	4.6284	0.004162	0.004231	0.004107	0.004167
Replicate 3	5.7949	2.3530	4.5547	0.004114	0.004176	0.004042	0.004111
Average concentration (g/g)							0.004123
Standard deviation (g/g)							0.000039

The qH $\{^{13}\text{C}\}$ NMR concentration of $^{13}\text{C}_6$ -ochratoxin A in Sample 1 at 400 MHz:

Mean I_c = (2.0000+2.0034+2.0127)/3 = 2.0054 (the mean I_c from the three replicates was used for all calculations)

	I_{an}			Concentration (g/g)			Overall concentrations (g/g)
	H(16-20)	H(3, 13)	H(4, 14)	H(16-20)	H(3, 13)	H(4, 14)	
Replicate 1	7.5459	3.1581	6.1775	0.004018	0.004204	0.004112	0.004111
Replicate 2	7.6525	3.1039	6.1581	0.004075	0.004132	0.004099	0.004102
Replicate 3	7.5998	3.1441	6.1484	0.004047	0.004185	0.004092	0.004108
Average concentration (g/g)							0.004107
Standard deviation (g/g)							0.000005

The ANOVA: Single factor comparison between qHNMR and GARP decoupling data for $^{13}\text{C}_6$ -ochratoxin A sample 1:

ANOVA: Single factor

SUMMARY

<i>Groups</i>	<i>Count</i>	<i>Sum</i>	<i>Average</i>	<i>Variance</i>
Proton	3	0.012368798	0.004122933	1.52E-09
GARP	3	0.012320612	0.004106871	2.31E-11

ANOVA

<i>Source of Variation</i>	<i>SS</i>	<i>df</i>	<i>MS</i>	<i>F</i>	<i>P-value</i>	<i>F crit</i>
Between groups	3.86969E-10	1	3.86969E-10	0.502141	0.51767401	7.708647
Within groups	3.08255E-09	4	7.70638E-10			
Total	3.46952E-09	5				

The concentration of $^{13}\text{C}_6$ -ochratoxin A (analyte) with maleic acid as external standard for Sample 2

Equation for calculating concentration (g/g) by quantitative NMR with an external standard:

$$[\text{analyte}] = \frac{I_{an}}{I_c} \cdot \frac{N_c}{N_{an}} \cdot \frac{\theta_{an}^{360}}{\theta_c^{360}} \cdot \frac{NS_c}{NS_{an}} \cdot \frac{MW_{an}}{MW_c} \cdot \frac{m_c}{m_c^{soln}} \cdot w_c$$

Where

I_{an} = integral of analyte

N_{an} = number of ^1H nuclei giving rise to integral of the analyte = 5 for H(16-20); 2 for H(3, 13); 4 for H(4, 14)

MW_{an} = molecular weight of analyte = 409.7 g/mol

NS_{an} = number of scans for analyte = 32

θ_{an}^{360} = 360° pulse for analyte = 51.5 μs

I_c = integral of standard

N_c = number of ^1H nuclei giving rise to integral of the standard = 2

MW_c = molecular weight of standard = 116.073 g/mol

m_c = mass of standard = 3.922 mg

NS_c = number of scans for standard t = 16 for ^1H -qNMR and 12 for $^1\text{H}\{^{13}\text{C}\}$ -qNMR

θ_c^{360} = 360° pulse for standard = 51.5 μs

m_c^{soln} = mass of standard solution = 1203.117 mg

w_c = purity of standard = 0.9989 g/g

No receiver gain correction was necessary as an RG of 181 was used for both analyte and standard.

The qHNMR concentration of $^{13}\text{C}_6$ -ochratoxin A in Sample 2 at 400 MHz:

Mean I_c = (2.0000+2.0008+2.0115)/3 = 2.0041 (the mean I_c from the three replicates was used for all calculations)

	I_{an}			Concentration (g/g)			Overall concentrations (g/g)
	H(16-20)	H(3, 13)	H(4, 14)	H(16-20)	H(3, 13)	H(4, 14)	
Replicate 1	3.1167	1.2725	2.4475	0.003575	0.003649	0.003509	0.003578
Replicate 2	3.1099	1.2808	2.4360	0.003567	0.003672	0.003493	0.003577
Replicate 3	3.1309	1.2758	2.4522	0.003591	0.003658	0.003516	0.003588
Average concentration (g/g)							0.003581
Standard deviation (g/g)							0.000006

The qH $\{^{13}\text{C}\}$ NMR concentration of $^{13}\text{C}_6$ -ochratoxin A in Sample 2 at 400 MHz:

Mean I_c = (2.0000+1.9826+1.9863)/3 = 1.9896 (the mean I_c from the three replicates was used for all calculations)

	I_{an}			Concentration (g/g)			Overall concentrations (g/g)
	H(16-20)	H(3, 13)	H(4, 14)	H(16-20)	H(3, 13)	H(4, 14)	
Replicate 1	4.1072	1.6970	3.2693	0.003556	0.003676	0.003541	0.003592
Replicate 2	4.0671	1.6881	3.2722	0.003524	0.003657	0.003544	0.003575
Replicate 3	4.1175	1.6974	3.3658	0.003568	0.003677	0.003537	0.003594
Average concentration (g/g)							0.003587
Standard deviation (g/g)							0.000010

The ANOVA: Single factor comparison between ^1H -qNMR and GARP decoupling data for $^{13}\text{C}_6$ -ochratoxin A sample 2:

ANOVA: Single factor

SUMMARY

<i>Groups</i>	<i>Count</i>	<i>Sum</i>	<i>Average</i>	<i>Variance</i>
Proton	3	0.010743638	0.003581	3.97E-11
GARP	3	0.010761294	0.003587	1.09E-10

ANOVA

<i>Source of Variation</i>	<i>SS</i>	<i>df</i>	<i>MS</i>	<i>F</i>	<i>P-value</i>	<i>F crit</i>
Between groups	5.19567E-11	1	5.2E-11	0.701001	0.449555	7.708647
Within groups	2.96472E-10	4	7.41E-11			
Total	3.48428E-10	5				

References:

1. Bates, J.; Bahadoor, A.; Cui, Y.; Meija, J.; Windust, A.; Melanson, J. E., Certification of Ochratoxin A Reference Materials: Calibration Solutions OTAN-1 and OTAL-1 and a Mycotoxin-Contaminated Rye Flour MYCO-1. *J. AOAC Int.* **2019**, *102*, 1-10.
2. Claridge, T. D. W., Correlations Through Space: The Nuclear Overhauser Effect. In *High-Resolution NMR Techniques in Organic Chemistry*, 2nd ed.; Elsevier: 2009; pp 315-380.
3. Reich, H. J. The Nuclear Overhauser Effect. <https://www.chem.wisc.edu/areas/reich/nmr/08-tech-02-noe.htm> (accessed March 30, 2020).